Article

Not peer-reviewed version

Neurotransmission Sex Dichotomy in the Rat Hypothalamic Paraventricular Nucleus in Health and Infantile Spasm Model

Dumitru Andrei Iacobas *, Jana Veliskova, Tamar Chachua, Chian-Ru Chern, Kayla Vieira, Sanda Iacobas, Libor Velisek

Posted Date: 27 March 2025

doi: 10.20944/preprints202503.2046.v1

Keywords: Adcy5; cholinergic synapse; dopaminergic synapse; GABAergic synapse; glutamatergic synapse: serotonergic synapse; synaptic vesicle cycle; transcriptomic network

Article

Neurotransmission Sex Dichotomy in the Rat Hypothalamic Paraventricular Nucleus in Health and Infantile Spasm Model

Dumitru A Iacobas [1,*], Jana Velíšková [2], Tamar Chachua [3], Chian-Ru Chern [3], Kayla Vieira [3], Sanda Iacobas [4] and Libor Velíšek [5]

[1] Personalized Genomics Laboratory, Undergraduate Medical Academy, School of Public and Allied Health, Prairie View A&M University, Prairie View, TX 77446, USA

[2] Departments of Cell Biology & Anatomy, Obstetrics and Gynecology, and Neurology, New York Medical College, Valhalla, NY 10595, USA; jana_veliskova@nymc.edu

[3] Department of Cell Biology & Anatomy, New York Medical College, Valhalla, NY 10595, USA; tamarchachua@gmail.com (T.C.); chianru_chern@nymc.edu (C.-R.C.); kvieira2@student.nymc.edu (K.V.)

[4] Department of Pathology, New York Medical College, Valhalla, NY 10595, USA; sandaiacobas@gmail.com

[5] Departments of Cell Biology & Anatomy, Pediatrics, and Neurology, New York Medical College, Valhalla, NY 10595, USA; libor_velisek@nymc.edu

* Correspondence: daiacobas@pvamu.edu

Abstract: We profiled the gene expressions in hypothalamic paraventricular nuclei of 12 male and 12 female pups from a standard rat model of infantile spasms to determine the sex dichotomy of the neurotransmission genomic fabrics. Infantile spasms were triggered in rat pups prenatally primed with two doses of betamethasone followed by postnatal repeated administration of N-methyl-D-aspartic acid to induce spasms. Publicly available microarray data were used to characterize each gene in each condition for both sexes by the independent transcriptomic features: average expression level, control of the transcript abundance, and expression correlation with each other gene. The study revealed substantial sex differences in the expression level, control, and inter-coordination of the investigated genes among the studied groups. The transcriptomic differences assist in providing a molecular explanation of the behavioral differences and development of infantile epilepsy spasm syndrome in the two sexes.

Keywords: Adcy5; cholinergic synapse; dopaminergic synapse; GABAergic synapse; glutamatergic synapse: serotonergic synapse; synaptic vesicle cycle; transcriptomic network

1. Introduction

This report presents an analysis of experimental data on the hypothalamic paraventricular nucleus (PVN) and complements a large study aiming to determine consequences of infantile spasms (infantile epilepsy spasm syndrome; IESS) on the neurotransmission transcriptome within the hypothalamic nuclei in a male and female rat model of IESS. The analyses encompassed the KEGG-constructed pathways: synaptic vesicle cycle (SVC), [1], and glutamatergic (GLU) [2], GABAergic (**GABA**) [3], cholinergic (**ACh**) [4], dopaminergic (**DA**) [5], and serotonergic (**5HT**) [6] synapses. Previously, we have shown that prenatal priming with betamethasone increases the occurrence of clinical spasms in the prenatal betamethasone-postnatal N-methyl-D-aspartic acid (NMDA) model and identified activation of several hypothalamic nuclei (i.e., arcuate nucleus and paraventricular nucleus) during the spasms [7,8]. Thus, we first studied the spasm-induced transcriptomic alterations in the hypothalamic arcuate nucleus (**ARC**) and the efficacy of two anti-IESS treatments [9,10].

IESS (formerly infantile spasms, also West Syndrome) represents a unique and devastating seizure syndrome of infancy [11,12]. IESS affects one out of each 3,200-3,400 infants with a yearly

 doi:10.20944/preprints202503.2046.v1

occurrence of approximately 1,700 new cases in the US [13]. The syndrome consists of (1) characteristic epileptic spasms during infancy (3-24 months of age), (2) interictal hypsarrhythmia (large amplitude, asynchronous waves) on the electroencephalogram (EEG), and (3) developmental or psychomotor arrest/delay [13]. IESS-specific FDA-approved first line therapy is hormonal (adrenocorticotropin; ACTH, or corticosteroids such as prednisone, prednisolone or methylprednisolone) or vigabatrin [14–16]. However, these treatments neither fully alleviate the condition nor are they free of serious side effects [17,18]. Many patients with IESS may die within the first years of life or suffer from permanent developmental deficits [19]. This poor prognosis necessitates a search for novel treatment targets. Interestingly, IESS has sex-preponderance affecting more boys than girls (from 1.5:1.0 to 1.1:1.0) [20–22].

We have developed a model of IESS in infant rats, which includes prenatal priming with betamethasone and an early postnatal trigger of spasms by NMDA, [7] that can be repetitive [23]. The spasms triggered by NMDA in the betamethasone primed rat brain are tightly linked to early development, are semiologically similar to spasms observed in human patients with IESS, share similar EEG patterns, and respond to ACTH, corticosteroids (methylprednisolone) or vigabatrin treatment [23–25]. This model has been independently reproduced and validated [26–28]. The disorganized EEG recordings seen in this model, as well as in the human condition of IESS [12], indicate altered brain circuitry, presumably caused by impaired inter-neuronal communication via neurotransmitters [9]. Our previous imaging studies indicated that the hypothalamus represents a critical hub that may participate in the control of spasms [7].

Among the brain regions, the hypothalamus is responsible for performing numerous neuroendocrine functions through the neuronal networks located in its specialized nuclei [15]. The paired paraventricular nuclei of the hypothalamus, located in the anterior hypothalamus adjacent to the sides of the third ventricle, are central to regulating the stress response and emotions leading to addictive behavior [14–16] as well as promoting satiety [17,18] through excitatory synaptic transmission circuits [17,18]. The PVN is also critical for the synthesis of vasopressin to regulate blood pressure, oxytocin for control of stress responses, and has connections to the brain stem to control sympathetic circuitry [19,29].

The PVN, consists of an intricate network of neurons interconnected by: cholinergic [20], dopaminergic [21], GABAergic [22], glutamatergic [7], and serotonergic [23] synapses, each classified according to the neurotransmitter used in the synaptic vesicle cycle [24]. GLU is a primary excitatory neurotransmitter [26] and GABA is the most abundant inhibitory [27] synapse in the mammalian central nervous system, and thus, both are associated with fundamental functions of the nervous system [28,29]. Other neurotransmitters and their corresponding synapses also play important roles in behavior. Accordingly, the **ACh** synapse facilitates learning, memory, and attention [30,31], the **DA** synapse controls learning, memory, motivation, and reward [32–34], and the **5HT** synapse is involved in learning and memory, emotion, abnormal mood, and cognition [35–37].

Given the inextricable link between synaptic sex-specific brain organization and behavior, development of neurological diseases suggest potentially distinct brain neuronal wirings, most likely related to organizational effects of sex hormones [38–40]. Among others, we have previously reported a substantial sex dichotomy in the gene networking and topology of the rat hypothalamic cytoskeleton [41], as well as in the myelination [41], and **GLU** and **GABA** synapse genomic fabrics [8].

In the present study at the time of the animal sacrifice on postnatal day (P) 16, their developmentally programmed sex differences are already irreversible. Although the gonads become active in males and females around P28-P30 (rat puberty), the males are exposed to gonadal steroids surges prenatally, and most importantly, to the neonatal testosterone surge between P0-P5. The role of sex hormones in modulating brain activity in epilepsy is well-documented (e.g. [30,31,42,43])

 doi:10.20944/preprints202503.2046.v1

2. Materials and Methods

2.1. Animals, Treatments and Tissue Collection

We used offspring of timed-pregnant Sprague Dawley rats (Taconic Farms,Germantown, NY) purchased on gestational day 8 (G8). Dams were housed in our AAALAC-accredited animal facility with free access to chow and water on the 12-hour light-dark cycle (lights on at 7:00 am). All experiments were approved by New York Medical College Institutional Animal Care and Use Committee (IACUC) and conform to the NIH Guide for the Care and Use of LaboratoryAnimals, 8th edition.

On their G15, 10 pregnant females, were injected twice with either saline or 0.4 mg/kg betamethasone phosphate (Sigma-Aldrich, St. Louis, MO). After birth on G23 (designated as P0), pups were weighted and sexed. Some of prenatal betamethasone-primed male and female pups received N-Methyl-D-Aspartic acid on P12, P13, and P15 to trigger spasms. Spasms were followed for 60 minutes after the trigger. Remainder of betamethasone-primed male and female pups was injected with corresponding volume of saline for control (no spasms). Animals were euthanized on P16 under deep CO_2 inhalation anesthesia, the pups were quickly perfused with ice-cold saline, the brain were removed, and the PVNs were dissected. The tissue was immediately snap frozen in dry ice for further processing. There were 6 groups of four samples according to their sex (M/F), saline/betamethasone (S/B) primed, and spasms presence (Y/N): MSN, FSN, MBN, FBN, MBY, and FBY (or analogously SN, BN, and BY for each sex). No more than male and two female pups from each litter entered the experiments, so that each group was composed of pups collected from two mothers.

2.2. Microarray and Data Processing

Total RNA extracted with Qiagen RNeasy mini-kit, concentration determined with NanoDrop ND-2000 Spectrophotometer and purity with Agilent RNA 6000 Nano kit in an Agilent 2100 Bioanalyzer. Total RNA was reverse transcribed in the presence of Cy3/Cy5 dUTP, and the incorporation of the fluorescent tags was determined with the NanoDrop. The arrays were scanned and primarily analyzed with an Agilent G4900DA SureScan Microarray Scanner Bundle (dual laser scanner + PC data system + Feature Extraction Software). The wet protocol and the raw data were deposited in the publicly accessible Gene Expression Omnibus databases [44–46].

All spots affected by local corruption or with foreground fluorescence less than twice the background in one microarray were disregarded and background subtracted foreground fluorescence signals were normalized to the median and results averaged for every set of spots probing redundantly the same gene. Normalization to the median gene expression provides comparable expression of individual genes across biological replicas, otherwise affected by the errors in sizing the samples. According our Genomic Fabric Paradigm [47]. Each quantifiable gene "in all samples was characterized by three independent features: *AVE* = average expression level (1), *REC* = relative expression control (2) and *COR* = expression correlation with each-other gene (3), defined by the formulas:

$$\forall i,j = 1 \div N \;\&\; \forall s = MSN, FSN, MBN, FBN, MBY, FBY$$

$$AVE_i^{(s)} \equiv \frac{1}{4}\sum_{k=1}^{4}\left(\frac{\propto_{i;k}^{(c)}{}^{(c)}}{\langle \alpha_{i;k}^{(c)} \rangle_{i;k}}\right) with\ a_i^{(c)} = \frac{1}{4}\sum_{k=1}^{4} \propto_{i;k}^{(c)} \quad (1)$$

$\propto_{i;k}^{(c)}$ is the background subtractd fluorescence of the spot probing that gene in replica k (=1,2,3,4) of sample s, $\langle \alpha_{i;k}^{(c)} \rangle$ is the net fluorescence of the median gene and $a_i^{(c)}$ is the average net fluorescence over all biological replicas.

 doi:10.20944/preprints202503.2046.v1

$$REC_i^{(c)} \equiv log_2\left(\frac{\langle REV_i^{(c)}\rangle}{REV_i^{(c)}}\right), where: \quad (2)$$

$$RCS_i^{(c)} \equiv \frac{\langle REV_i^{(c)}\rangle}{REV_i^{(c)}} = \text{ the relative control strength} \quad (2a)$$

$$\langle REV_i^{(c)}\rangle \text{ is the median } REV \quad (2b)$$

$$REV_i^{(c)} \equiv \frac{\sigma_i^{(c)}}{2AVE_i^{(c)}}\left(\sqrt{\frac{r_i}{\chi^2(\beta;r_i)}} - \sqrt{\frac{r_i}{\chi^2(1-\beta;r_i)}}\right) \quad (2c)$$

REC is computed using the midinterval of the χ^2 distribution of the coeficient of variation of the normalized expression levels across biological replicas. *COR* is the pair-wise Pearson correlation coefficient of the (log_2) of the normalized expression levels of the two genes [48]. The expression controls in two conditions of the same sex or one condition in both sexes were compared through the fold-change (*FC*), negative for down-regulation:

$$FC_i^{(compared\ vs\ reference)} = \begin{cases} \frac{RCS_i^{(compared)}}{RCS_i^{(reference)}}, if\ RCS_i^{(compared)} > RCS_i^{(reference)} \\ -\frac{RCS_i^{(reference)}}{RCS_i^{(compared)}}, if\ RCS_i^{(compared)} \leq RCS_i^{(reference)} \end{cases} \quad (2d)$$

$$COR_{i,j}^{(c)} \equiv correl\left(log_2\left(\frac{\propto_{i;k}^{(c)}{}^{(c)}}{\langle\alpha_{i;k}^{(c)}\rangle_{i;k}}\right), log_2\left(\frac{\propto_{j;k}^{(c)}{}^{(c)}}{\langle\alpha_{j;k}^{(c)}\rangle_{i;k}}\right)\right) \quad (3)$$

COR analysis [48] was used to identify the $p < 0.05$ significant inter-gene synergistic/antagonistic/independent expressions. This analysis is the prerequisite to determine the most active transcriptomic networks interlinking (here) the genes involved in neurotransmission. It is important to remember that the statistically significant positive correlation means that expression of either gene stimulates the expression of the other, the negative correlation points out the opposite tendency, while independence reveals total decoupling of the encoded products of the two genes. *COR* analysis can also be used to test the validity of the wiring in the KEGG-constructed pathways under normal condition (M/F)SN and quantify their remodeling in the imposed conditions (M/F)BN and (M/F)BY. Moreover, by comparing the results in males and females, one can find whether the documented effects of the sex hormones on neurotransmission [49–51] should include the differences in the expression control and organization of gene transcriptomic networks beyond differential expression levels.

The transcriptomic influential powers of individual genes computed using the measure termed "Gene Commanding Height", *GCH* that combines the expression control and the median of the expression coordination with each-other genes:

$$GCH_i^{(c)} \equiv exp\left(REC_i^{(c)} + \langle\left(2COR_{i,j}^{(c)}\right)^2\rangle_j\right) \quad (4)$$

The top gene (highest GCH) in each condition was termed Gene Master Regulator (GMR). Pending of the type of genetic manipulation, the GMR might be the most legitimate target for the gene therapy aiming to destroy or to stimulate the proliferation of the most abundant clone in that condition [52].

Expression of a gene is considered as significantly regulated when comparing BN with SN and BY with BN for each sex or as significantly different when comparing the two sexes within the same condition, if it satifies the composite criterion (4). for the absolute fold-change $|x|$ and the p-value of the heteroscedastic *t*-test of means' equality [53]:

 doi:10.20944/preprints202503.2046.v1

$$\begin{cases} \left| x_i^{(compared\ vs\ reference)} \right| > CUT_i^{(compared\ vs\ reference)} \\ p_i^{(compared\ vs\ reference)} < 0.05 \end{cases} \quad (5)$$

where:

$$x_i^{(compared\ vs\ reference)} = \begin{cases} \dfrac{AVE_i^{(compared)}}{AVE_i^{(reference)}}, if\ AVE_i^{(compared)} > AVE_i^{(reference)} \\ -\dfrac{AVE_i^{(reference)}}{AVE_i^{(compared)}}, if\ AVE_i^{(compared)} \le AVE_i^{(reference)} \end{cases} \quad (5a)$$

$$CUT_i^{(compared\ vs\ reference)} = 1 + \sqrt{\frac{2}{100}\left(\left(REV_i^{(compared)}\right)^2 + \left(REV_i^{(reference)}\right)^2\right)} \quad (5b)$$

2.3. KEGG-Constructed Functional Neurotransmission Pathways

The analyses were directed towards genes associated with the KEGG (Kyoto Encyclopedia of Genes and Genomes, [54]) constructed pathways: synaptic vesicle cycle (SVC, denoted by "0" in the column "Path" of tables below), and glutamatergic (GLU, "1"), GABAergic (GABA, "2"), cholinergic (ACh, "3"), dopaminergic (DA, "4") and serotonergic (5HT, "5") synapse [1–6]. We were able to quantify properly in all samples: 69 out of 80 the KEGG listed SVC genes, 90 out of 115 GLU genes, 67 out of 90 GABA genes, 80 out of 113 ACh genes, 111 out of 132 DA genes, and 71 out of 130 5HT genes. The pathways are partially overlapping with several genes shared by two or more pathways. For instance, *Gnai2* is part of all five types of synapse and *Mapk3* of the glutamatergic, cholinergic, and serotonergic synapses.

3. Results

3.1. There Is Little Sex Dichotomy of the Most Highly Expressed Neurotransmission Genes

Table 1 presents the *top* five genes associated with the functional pathways: SVC ("0"), GLU ("1"), GABA ("2"), ACh ("3"), DA ("4") and 5HT ("5") that exhibited the largest expression levels *in each* sex in all three conditions. Of note is almost unchanged gene hierarchy according to their normalized *(to the median gene)* expression levels, although their expression was a little higher in females (*See* Table S1 in Supplementary Material for the ratio "x" of the (M/F) expression levels according to definition (5a)). For instance, with respect to the median gene expression, the DA gene Caly has 126x more transcripts than the median gene in male SN (but 195x in female SN), 139x in male BN (but 143x in female BN), and 126x in male BY (but 155x in female BY). However, although these top five genes in the analyzed neurotransmission functional pathways were practically not differentially expressed, other neurotransmission genes presented statistically significant differential expression between the two sexes, as shown in Figure 2. For comparison, the table includes also the non-neurotransmission genes (no number in the "Path" column) with the largest expression levels (*Cst3, Rpl41*), indicating that the neurotransmission genes are among the most highly expressed in the PVN transcriptome.

Table 1. The top five most expressed neurotransmission genes in the PVN of the two **sexes subjected to each of the three conditions.** The average expression levels were normalized to the expression of the median gene in that condition for each sex. Note the similarity of the gene hierarchy in each group of samples.

 doi:10.20944/preprints202503.2046.v1

	Top 5 expressed neurotransmission genes		MALE			FEMALE		
Gene	**Description**	**PATH**	**SN**	**BN**	**BY**	**SN**	**BN**	**BY**
Caly	**calcyon neuron-specific vesicular protein**	4	**126**	139	126	195	143	155
Gabarapl1	GABA(A) receptor-associated protein like 1	2	104	112	80	69	108	129
Ap2m1	adaptor-related protein complex 2, mu 1 subunit	0	96	110	89	125	112	122
Calm2	calmodulin 2	4	72	70	60	60	75	72
Hap1	huntingtin-associated protein 1	2	63	63	67	73	72	73
Caly	**calcyon neuron-specific vesicular protein**	4	126	139	126	**195**	143	155
Ap2m1	adaptor-related protein complex 2, mu 1 subunit	0	96	110	89	125	112	122
Mapk3	mitogen activated protein kinase 3	135	59	64	67	85	68	68
Gnai2	guanine nucleotide binding protein (G protein), alpha inhibiting activity polypeptide 2	12345	57	64	57	75	64	74
Hap1	huntingtin-associated protein 1	2	63	63	67	73	72	73
Caly	**calcyon neuron-specific vesicular protein**	4	126	**139**	126	195	143	155
Gabarapl1	GABA(A) receptor-associated protein like 1	2	104	112	80	69	108	129
Ap2m1	adaptor-related protein complex 2, mu 1 subunit	0	96	110	89	125	112	122
Calm2	calmodulin 2	4	72	70	60	60	75	72
Gnai2	guanine nucleotide binding protein (G protein), alpha inhibiting activity polypeptide 2	12345	57	64	57	75	64	74
Caly	**calcyon neuron-specific vesicular protein**	4	126	139	126	195	**143**	155
Ap2m1	adaptor-related protein complex 2, mu 1 subunit	0	96	110	89	125	112	122
Gabarapl1	GABA(A) receptor-associated protein like 1	2	104	112	80	69	108	129
Calm2	calmodulin 2	4	72	70	60	60	75	72
Hap1	huntingtin-associated protein 1	2	63	63	67	73	72	73
Caly	calcyon neuron-specific vesicular protein	4	126	139	**126**	195	143	155
Ap2m1	adaptor-related protein complex 2, mu 1 subunit	0	96	110	89	125	112	122
Gabarapl1	GABA(A) receptor-associated protein like 1	2	104	112	80	69	108	129
Mapk3	mitogen activated protein kinase 3	135	59	64	67	85	68	68
Hap1	huntingtin-associated protein 1	2	63	63	67	73	72	73
Caly	**calcyon neuron-specific vesicular protein**	4	126	139	126	195	143	**155**
Gabarapl1	GABA(A) receptor-associated protein like 1	2	104	112	80	69	108	129
Ap2m1	adaptor-related protein complex 2, mu 1 subunit	0	96	110	89	125	112	122
Gnai2	guanine nucleotide binding protein (G protein), alpha inhibiting activity polypeptide 2	12345	57	64	57	75	64	74
Hap1	huntingtin-associated protein 1	2	63	63	67	73	72	73
Cst3	cystatin C		**172**	187	**172**	222	**203**	206
Rpl41	ribosomal protein L41		162	**189**	161	**248**	188	**225**

3.2. Sex Dichotomy in the Expression Control in the Three Conditions and Control Alteration by IS

Tables 2 and 3 present the most and the least controlled neurotransmission genes in the paraventricular nodes of both sexes in all three conditions. Positive REC scores indicate how many times a gene is under a stricter controlled than the median gene, while a negative REC indicates a less controlled gene that the median of that group of samples. The most controlled genes (highest positive RECs) are most likely critical for cell survival and phenotypic expression, while the least controlled genes might be essential for the cell adaptation to the environmental changes. Supplementary Tables S2a and S3a list the ratios of the Relative Control Strength (RCS) scores of the same genes between the two sexes in all three conditions, while Supplementary Tables S2b and S3b the ratios of the RCS in YS with respect to NS for each sex.

 doi:10.20944/preprints202503.2046.v1

Table 2. The most controlled neurotransmission genes in the PVN of the two sexes subjected to each of the three conditions. Note the alteration of the normal hierarchy of controlled gens in (M/F)NS and (M/F)BY conditions and the substantial differences between the two sexes in all three conditions. For comparison, the table includes the RECs of the most controlled non-neurotransmission genes (no number in the "Path" column): *Erg88*, *Erap1*, *Tmem238*, *Cul7*, *Oxsr1*, and *Tsc2*.

	Top 5 most controlled neurotransmission genes		MALE			FEMALE		
Gene	Description	PATH	SNS	BNS	BYS	SNS	BNS	BYS
Pik3r2	**phosphoinositide-3-kinase, regulatory subunit 2 (beta)**	3	**3.52**	1.04	0.82	0.83	0.75	0.73
Atp6v0b	ATPase, H+ transporting, lysosomal V0 subunit B	0	2.40	-0.59	1.22	1.01	0.12	-0.02
Calml4	calmodulin-like 4	4	2.15	-0.61	0.65	-0.56	-0.02	-0.71
Ppp1ca	protein phosphatase 1, catalytic subunit, alpha isozyme	4	2.13	0.55	1.12	1.16	2.00	1.32
Atp6v1g2	ATPase, H+ transporting, lysosomal V1 subunit G2	0	1.95	-0.32	0.67	0.06	0.87	1.39
Abat	**4-aminobutyrate aminotransferase**	2	0.38	1.52	1.63	**3.58**	1.81	0.33
Gabbr1	gamma-aminobutyric acid (GABA) B receptor 1	2	-0.26	0.72	0.75	2.87	0.15	1.23
Slc6a7	solute carrier family 6 (neurotransmitter transporter), member 7	0	1.08	-0.01	1.01	2.82	-0.08	1.63
Chrnb4	cholinergic receptor, nicotinic, beta 4 (neuronal)	3	0.87	0.09	0.40	2.75	0.60	0.11
Gnal	GTP-binding protein Golf alpha subunit	4	0.83	-0.98	-0.45	2.66	-0.28	-0.48
Pik3r5	**phosphoinositide-3-kinase, regulatory subunit 5**	3	-0.25	**2.42**	1.25	0.94	-1.19	1.17
Atp2a2	ATPase, Ca++ transporting, cardiac muscle, slow twitch 2	0	0.60	2.18	0.81	-0.60	1.53	0.94
Ppp2r5e	protein phosphatase 2, regulatory subunit B', epsilon isoform	4	0.76	2.04	2.08	-0.44	0.85	0.47
Ppp2r3c	protein phosphatase 2, regulatory subunit B'', gamma	4	1.70	1.85	0.72	-0.32	0.10	1.20
Slc38a5	solute carrier family 38, member 5	2	1.94	1.81	0.50	-0.09	-0.88	0.94
Grm8	**glutamate receptor, metabotropic 8**	1	0.25	-0.24	1.81	0.47	**2.70**	0.70
Cpne3	copine III	0	0.23	0.68	0.58	-0.98	2.39	-0.20
Atp6v1h	ATPase, H+ transporting, lysosomal V1 subunit H	0	0.80	1.55	0.50	-0.24	2.30	0.57
Gls	glutaminase (Gls), nuclear gene encoding mitochondrial protein	12	0.04	1.07	1.27	-1.34	2.19	0.76
Gabarapl2	GABA(A) receptor-associated protein like 2	2	0.66	0.62	1.10	-1.40	2.09	1.43
Th	**tyrosine hydroxylase**	4	-1.77	-0.50	**3.71**	0.05	-0.14	-0.16
Maoa	monoamine oxidase A	45	0.59	0.53	2.62	1.17	0.93	-0.42
Mapk10	mitogen activated protein kinase 10	4	0.97	0.30	2.35	-1.84	-0.04	0.44
Scn1a	sodium channel, voltage-gated, type I, alpha	4	-0.30	0.69	2.29	1.00	-0.67	0.30
Gabrg1	gamma-aminobutyric acid (GABA) A receptor, gamma 1	2	0.24	0.04	2.22	0.79	1.76	-0.87
Trpc1	**transient receptor potential cation channel, subfamily C, member 1**	15	0.57	0.98	1.87	-1.06	0.64	**4.87**
Gng10	guanine nucleotide binding protein (G protein), gamma 10	12345	0.56	1.08	0.11	0.05	1.38	2.79
Gng8	guanine nucleotide binding protein (G protein), gamma 8	1245	0.20	0.37	0.40	0.78	-0.18	2.58
Raf1	v-raf-leukemia viral oncogene 1	5	1.05	1.68	0.68	0.98	-0.64	2.21
Atp6v0a1	ATPase, H+ transporting, lysosomal V0 subunit A1	0	-0.21	0.11	1.68	-0.69	2.06	2.04
Erg28	**ergosterol biosynthesis 28 homolog**		**4.19**	0.52	-0.60	-0.03	1.22	0.24
Erap1	**endoplasmic reticulum aminopeptidase 1**		0.30	0.62	0.53	**4.87**	1.22	1.36
Tmem238	**transmembrane protein 238**		1.49	**5.32**	1.25	1.45	0.76	0.42
Cul7	**cullin-7**		0.67	0.74	0.96	-0.04	**4.22**	1.70
Oxsr1	**oxidative-stress responsive 1**		0.57	0.23	**4.33**	2.01	2.13	-0.12
Tsc2	**tuberous sclerosis 2**		-0.68	1.69	0.89	-0.11	1.20	5.98

One of the most controlled neurotransmission gene in the IS female PVN, *Gng10*, is part of all five types of synapses analyzed in this study. Of note are the substantial differences between the two sexes in all three conditions as well as the switch from very controlled in (M/F)SN to less controlled in (M/F)BN of *Atp6v0b*, *Calml4*, and *Atp6v1b*. Interestingly, the dopaminergic gene, *Th*, with a very loose control in male SN became strictly controlled in the condition of spasms.

 doi:10.20944/preprints202503.2046.v1

Table 3. The least controlled neurotransmission genes in the PVN of the two sexes subjected to all three conditions. Note the alteration of the normal hierarchy of controlled gens when BNS and BYS conditions and the substantial differences between the two sexes in all three conditions. For comparison, the table includes also the least controlled non-neurotransmission genes in each group of samples: *C11h21orf91*, *Snx5*, *Pddc1*, *Mobp*, *Pfk1*, and *Ptgds.*

	Top 5 least controlled neurotransmission genes		MALE			FEMALE		
Gene	**Description**	**PATH**	**SNS**	**BNS**	**BYS**	**SNS**	**BNS**	**BYS**
Calm1	**calmodulin 1**	4	**-2.05**	-0.87	-1.41	-1.27	-0.56	-0.30
Alox15	arachidonate 15-lipoxygenase	5	-2.04	-0.40	-1.20	-0.03	-1.23	-1.47
Th	tyrosine hydroxylase	4	-1.77	-0.50	3.71	0.05	-0.14	-0.16
Plcb1	phospholipase C, beta 1 (phosphoinositide-specific)	1345	-1.73	-1.61	-1.06	-0.27	-1.28	-1.58
Clock	clock circadian regulator	4	-1.48	-2.33	-1.76	-1.10	-1.61	-1.80
Mapk10	**mitogen activated protein kinase 10**	4	0.97	0.30	2.35	**-1.84**	-0.04	0.44
Gna11	guanine nucleotide binding protein, alpha 11	3	-0.54	-1.47	-1.16	-1.76	-0.62	-1.41
Gabarapl1	GABA(A) receptor-associated protein like 1	2	-0.72	-0.64	-0.90	-1.74	-0.66	-0.53
Rims1	regulating synaptic membrane exocytosis 1	0	-1.17	-1.73	-1.37	-1.69	-1.41	-1.67
Map2k1	mitogen activated protein kinase kinase 1	35	-0.51	0.19	0.57	-1.64	1.03	-0.19
Drd2	**dopamine receptor D2**	4	-0.63	**-2.45**	-1.42	-0.74	-1.59	-1.74
Slc6a12	solute carrier family 6 (neurotransmitter transporter), member 12	02	-0.58	-2.35	-1.35	-0.61	-1.29	-1.62
Clock	clock circadian regulator	4	-1.48	-2.33	-1.76	-1.10	-1.61	-1.80
Alox12b	arachidonate 12-lipoxygenase, 12R type	5	-1.16	-2.25	-1.39	-0.27	-1.53	-1.66
Gnb3	guanine nucleotide binding protein (G protein), beta polypeptide 3	12345	-0.88	-2.24	-1.57	-0.96	-1.56	-1.81
Creb3	**cAMP responsive element binding protein 3**	34	0.47	0.61	0.33	0.41	**-2.71**	0.13
Gng5	guanine nucleotide binding protein (G protein), gamma 5	12345	0.65	0.52	1.23	0.40	-2.22	1.47
Camk2b	calcium/calmodulin-dependent protein kinase II beta	34	0.90	-0.60	0.39	-1.08	-2.15	-0.05
Akt1	v-akt murine thymoma viral oncogene homolog 1	34	0.46	-0.23	0.29	-0.46	-2.15	-0.87
Slc1a3	solute carrier family 1 (glial high affinity glutamate transporter), member 3	01	-0.23	-0.48	-0.77	0.23	-2.07	-0.17
Clock	**clock circadian regulator**	4	-1.48	-2.33	**-1.76**	-1.10	-1.61	-1.80
Gria2	glutamate receptor, ionotropic, AMPA 2	14	0.28	-0.51	-1.64	-1.18	0.77	-0.32
Htr7	5-hydroxytryptamine (serotonin) receptor 7, adenylate cyclase-coupled	5	-0.94	-2.17	-1.60	-0.78	-1.66	-1.71
Unc13b	unc-13 homolog B (C. elegans)	0	-1.07	-2.22	-1.60	-0.24	-1.63	-1.78
Akt2	v-akt murine thymoma viral oncogene homolog 2	34	-0.94	-2.14	-1.57	-1.08	-1.29	-1.65
Grin1	**glutamate receptor, ionotropic, N-methyl D-aspartate 1**	1	-0.79	-1.87	-1.40	-0.45	-1.41	**-1.87**
Gnaq	guanine nucleotide binding protein (G protein), q polypeptide	1345	-1.04	-1.89	-1.46	-0.21	-1.19	-1.87
Chrna7	cholinergic receptor, nicotinic, alpha 7 (neuronal)	3	-1.38	-2.01	-1.57	-0.91	-1.36	-1.87
Cyp2c11	cytochrome P450, subfamily 2, polypeptide 11	5	0.54	-1.33	-0.99	0.15	-1.04	-1.86
Gnb3	guanine nucleotide binding protein (G protein), beta polypeptide 3	12345	-0.88	-2.24	-1.57	-0.96	-1.56	-1.81
C11h21orf91	similar to human chromosome 21 open reading frame 91		-3.67	-1.31	-0.28	-1.85	-0.38	-0.57
Snx5	sorting nexin 5		1.21	1.97	0.58	-2.66	0.96	1.13
Pddc1	Parkinson disease 7 domain containing 1		-0.54	-3.69	-0.12	0.57	0.05	-0.73
Mobp	myelin-associated oligodendrocyte basic protein		-1.63	-2.36	-0.78	-1.62	-3.09	-0.38
Pfkl	phosphofructokinase, liver		0.90	1.05	-2.67	-1.32	-1.14	-0.42
Ptgds	prostaglandin D2 synthase (brain)		-2.57	-1.93	-1.67	-1.17	-0.78	-3.49

We believe that the reason why expressions of some genes were left free to fluctuate is to provide adaptation to the changes of the environmental conditions. *Gnb3* and *Gng5* were the most flexibly expressed genes in the BNS condition in male, respective female PVNs that are included in all five synapse pathways.

Figure 1 illustrates the substantial sex differences in the gene expression control by plotting the RECs of the most (1a) and the least (1b) controlled genes in the three conditions.

 doi:10.20944/preprints202503.2046.v1

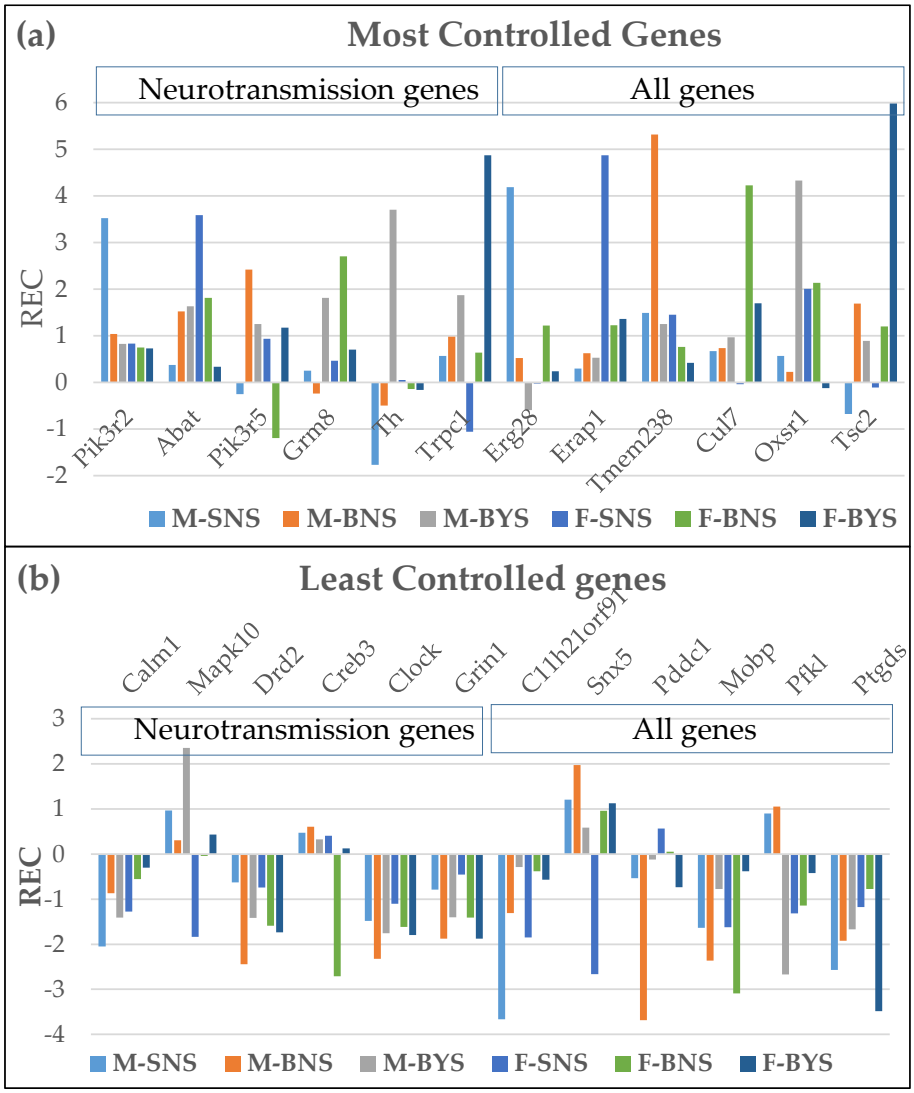

Figure 1. Relative Expression Control of the extreme genes.

3.3. Sex Differences in the Unaltered State of the Six Neurotransmission Pathways

Figure 2 presents the statistically significant (i.e. satisfying the composite criterion of $p < 0.05$ + absolute expression ratio > CUT) differential expression of the SVC (a), GLU (b), GABA (c), ACh (d), DA (e) and 5HT (f) pathways' genes between males and females in the unaltered state (SN) of the paraventricular hypothalamic nucleus. In this figure, the female transcriptome is the reference and male's is the referred.

 doi:10.20944/preprints202503.2046.v1

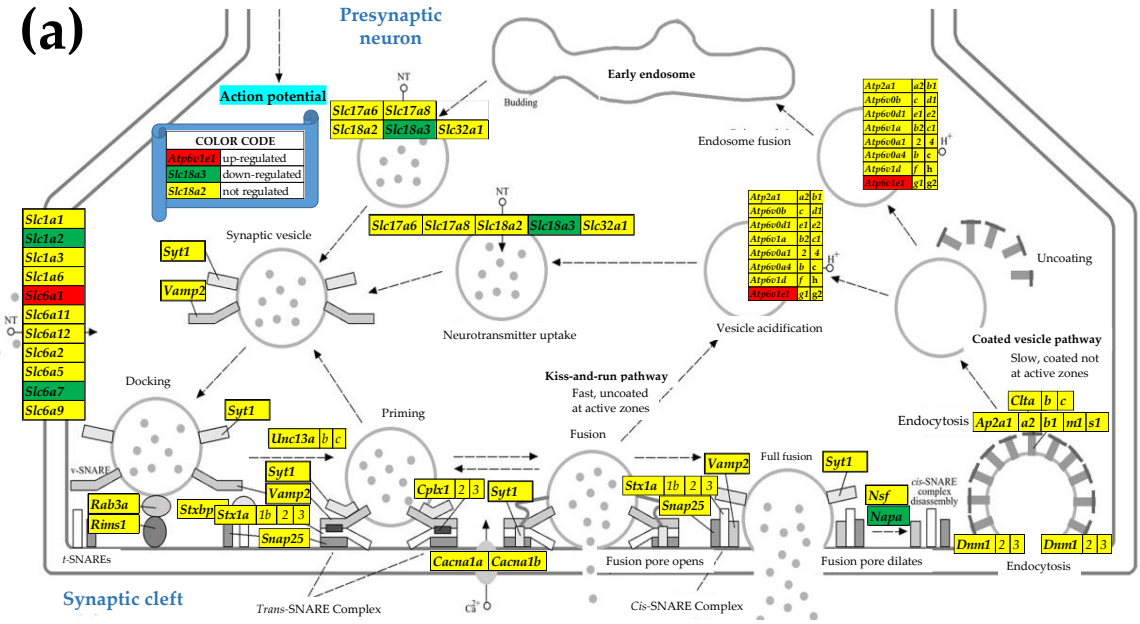

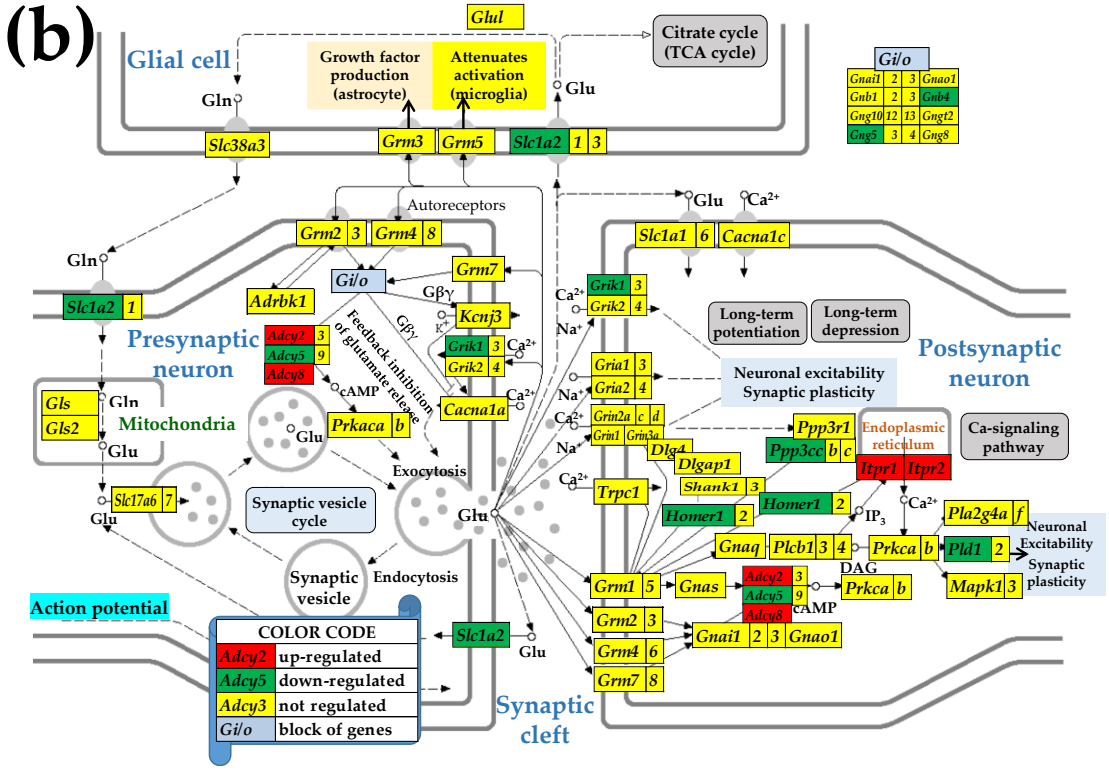

 doi:10.20944/preprints202503.2046.v1

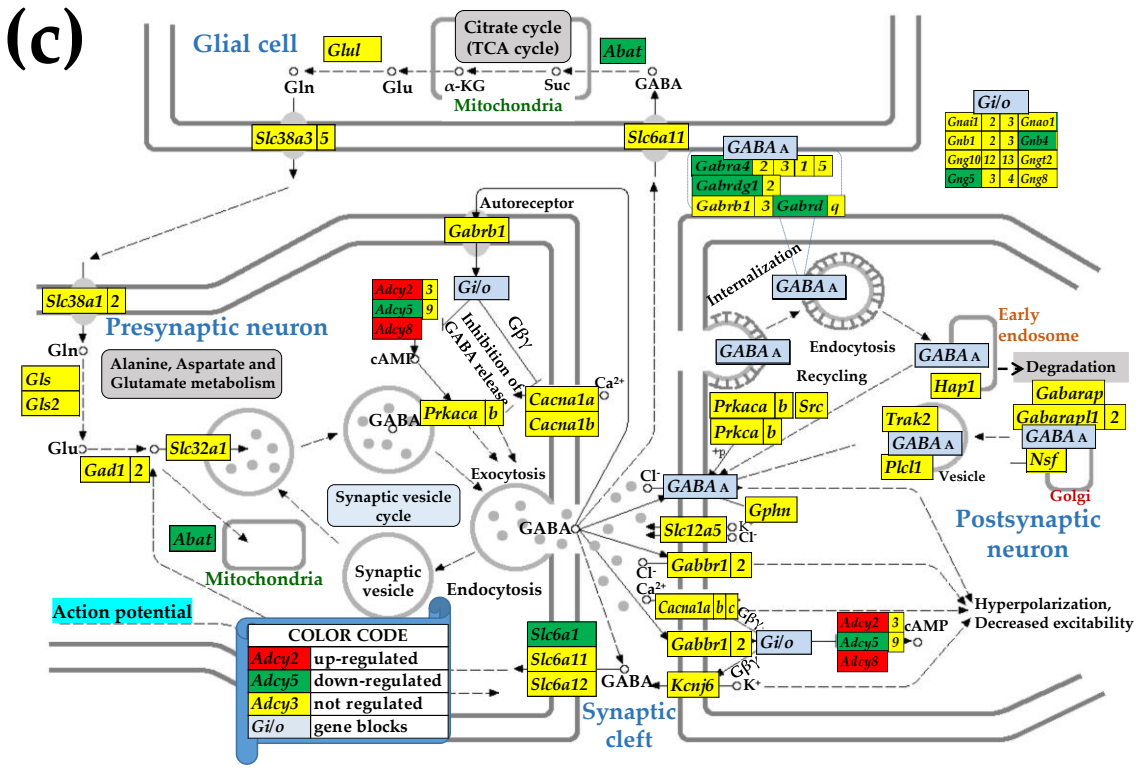

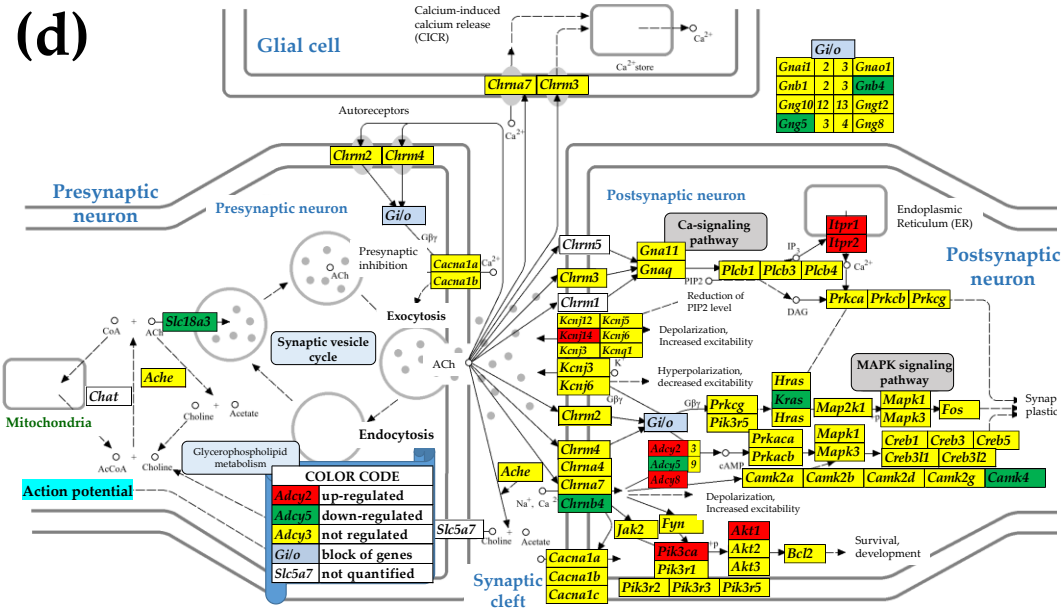

 doi:10.20944/preprints202503.2046.v1

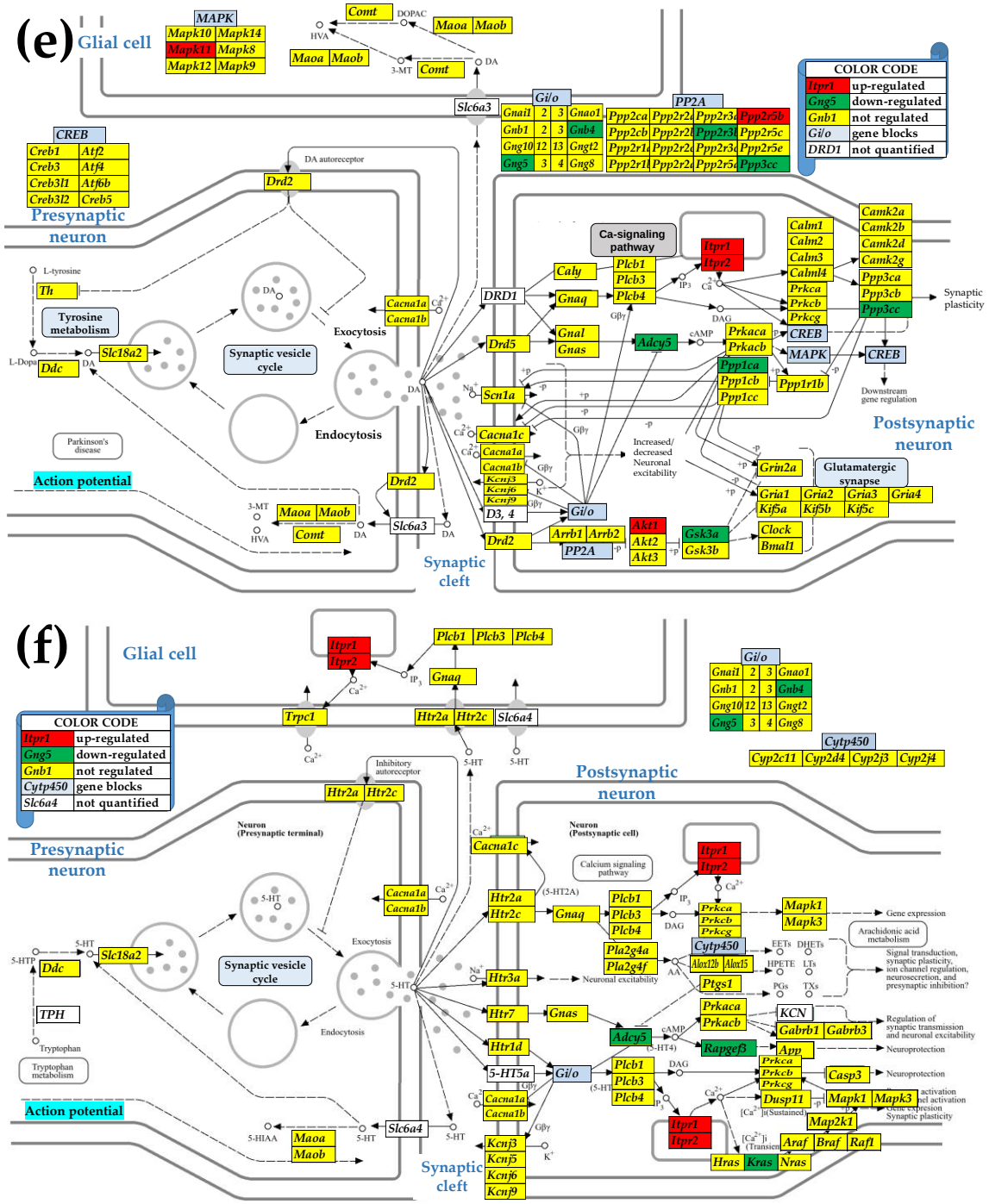

Figure 2. Sex differences in the unaltered (SN) state of the KEGG-constructed pathways: (**a**) Synaptic Vesicle Cycle, (**b**) Glutamatergic Synapse, (**c**) GABAergic, (**d**) Cholinergic, (**e**) Dopaminergic and (**f**) Serotonergic synapse in the PVN of male and female. Red/green background of the gene symbols indicates whether that gene was significantly over/under expressed in the male's with respect to the female's tissue, while yellow background indicates that the expression difference was not significant. Differentially expressed genes: *Abat* (4-aminobutyrate aminotransferase), *Adcy2/5/8* (adenylate cyclase 2/5/8), *Akt1* (v-akt murine thymoma viral oncogene homolog 1), *Atp6v1c1* (ATPase, H+ transporting, lysosomal V1 subunit C1), *Chrnb4* (cholinergic receptor, nicotinic, beta 4 (neuronal)), *Gabra4/d/g1* (gamma-aminobutyric acid (GABA) A receptor, alpha 4/delta/gamma1), *Gnb4* (guanine nucleotide binding protein (G protein), beta polypeptide 4), *Gng5* (guanine nucleotide binding protein (G protein), gamma 5), *Grik1* (glutamate receptor, ionotropic, kainate 1), *Homer1* (homer homolog 1 (Drosophila)), *Itpr1/2* (inositol 1,4,5-trisphosphate receptor, type 1/2), *Kcnj14* (potassium inwardly-rectifying channel, subfamily J, member 14), *Kras* (Kirsten rat sarcoma viral oncogene), *Mapk11* (mitogen-activated protein kinase 11), *Napa* (N-ethylmaleimide-sensitive factor attachment protein, alpha), *Pik3ca*

 doi:10.20944/preprints202503.2046.v1

(phosphoinositide-3-kinase, catalytic, alpha polypeptide), *Pld1* (phospholipase D1), *Ppp1ca* (protein phosphatase 1, catalytic subunit, alpha isozyme), *Ppp3cc* (protein phosphatase 3, catalytic subunit, gamma isozyme), *Slc18a3* (solute carrier family 18 (vesicular acetylcholine transporter), member 3), *Rapgef3* (Rap guanine nucleotide exchange factor (GEF) 3), *Slc1a2* (solute carrier family 1 (glial high affinity glutamate transporter), member 2), *Slc18a3* (solute carrier family 18 (vesicular acetylcholine transporter), member 3, *Slc6a1/7* (solute carrier family 6 (neurotransmitter transporter), member 1/7).

3.4. Sex Differences Between the Significantly Regulated SVC Genes in the PVN by the Induction of Spasms in the Betamethasone-Primed Rats

Figure 3 presents the statistically significant ($p < 0.05$, absolute fold-change > CUT) regulations in the SVC functional pathway following induction of the spasms in the betamethasone-primed state (BYS/BNS) of the PVN of male and female rats.

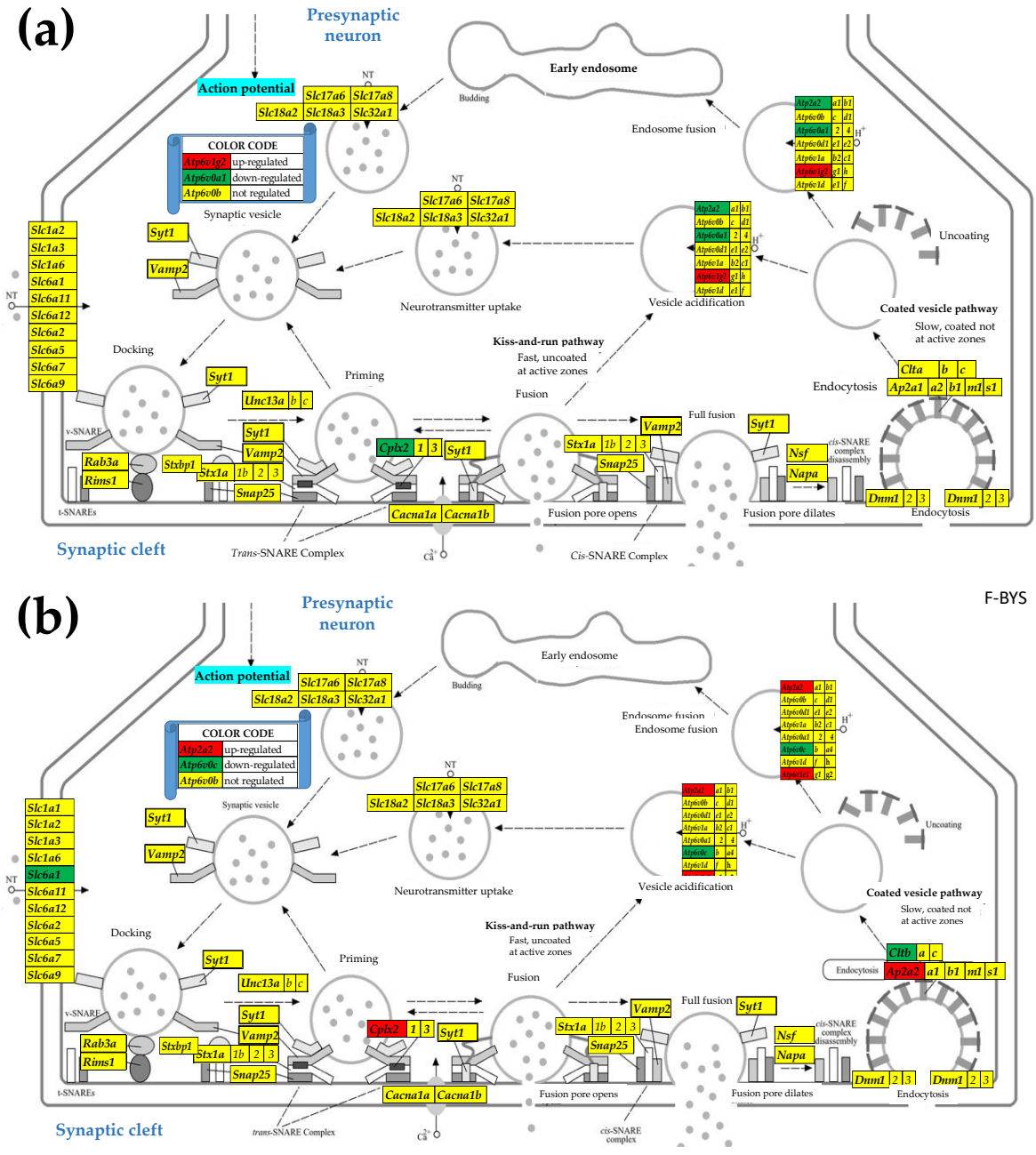

Figure 3. Sex differences in the regulome of the KEGG-constructed Synaptic Vesicle Cycle (SVC) in of the betamethasone-primed PVN following induction of the spasms. (**a**) Male rats. (**b**) Female rats. Red/green background of the gene symbols indicates whether that gene was significantly over/under expressed in the

 doi:10.20944/preprints202503.2046.v1

male's with respect to the female's tissue, while yellow background indicates that the expression difference was not significant. Differentially expressed genes: *Ap2a2* (adaptor-related protein complex 2, alpha 2 subunit), *Atp2a2* (ATPase, Ca++ transporting, cardiac muscle, slow twitch 2), *Atp6v0c* (ATPase, H+ transporting, lysosomal V0 subunit C), *Atp6v1c1/g2, Cplx2* (complexin 2), *Slc6a1.*

Out of the 69 quantified SVC genes, one was up regulated in males while four were upregulated in females. Three SVC genes were down-regulated in males versus two in females. Interestingly, two down-regulated genes in males, *Atp2a2* and *Cplx2* were up-regulated in females, indicating opposite effects of triggering the infantile spasms in the two sexes.

3.5. Sex Differences Between the Significantly Regulated GLU Genes in the PVN by the Induction of Infantile Spasms in the Betamethasone-Primed Rats

Figure 4 presents the statistically significant ($p < 0.05$, absolute fold-change > CUT) regulations in the GLU functional pathway following induction of the spasms in the betamethasone-primed state (BYS/BNS) of the PVN of male and female rats. Out of the 90 quantified GLU genes, four genes were up-regulated and three were down-regulated in males compared to two up-regulated and one down-regulated in females. Interestingly, *Adcy5*, included in all five synaptic pathways, was down-regulated by IS in males but up-regulated in females, indicating opposite effects of IS on the two sexes.

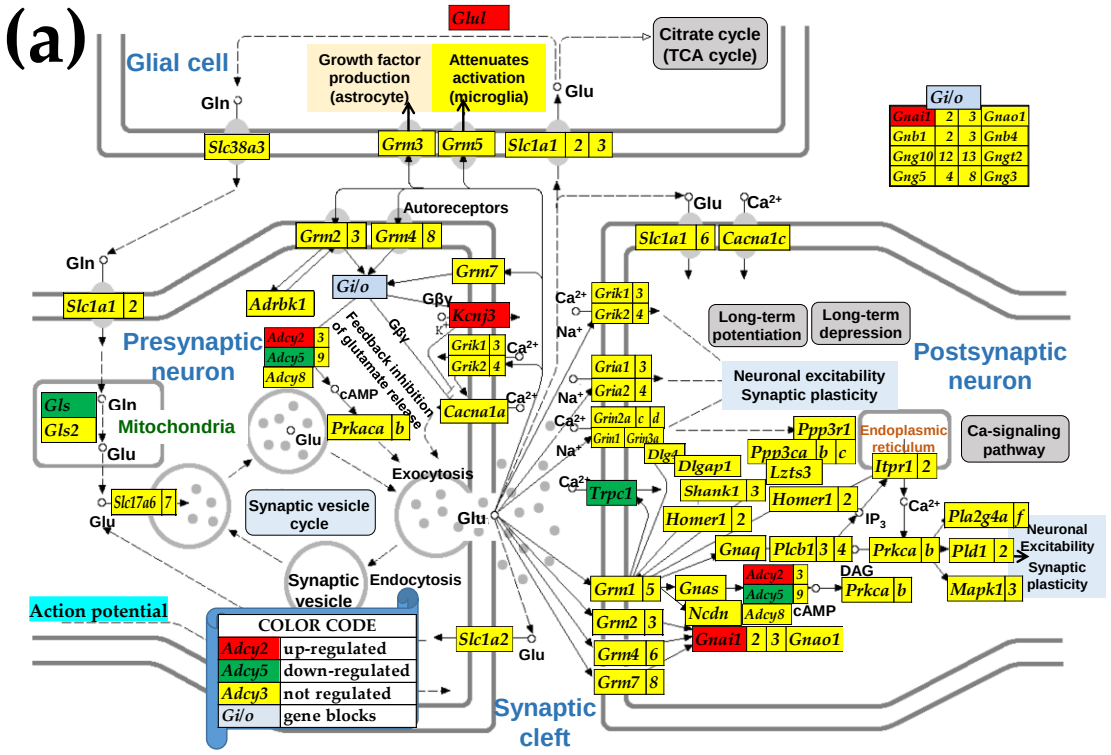

 doi:10.20944/preprints202503.2046.v1

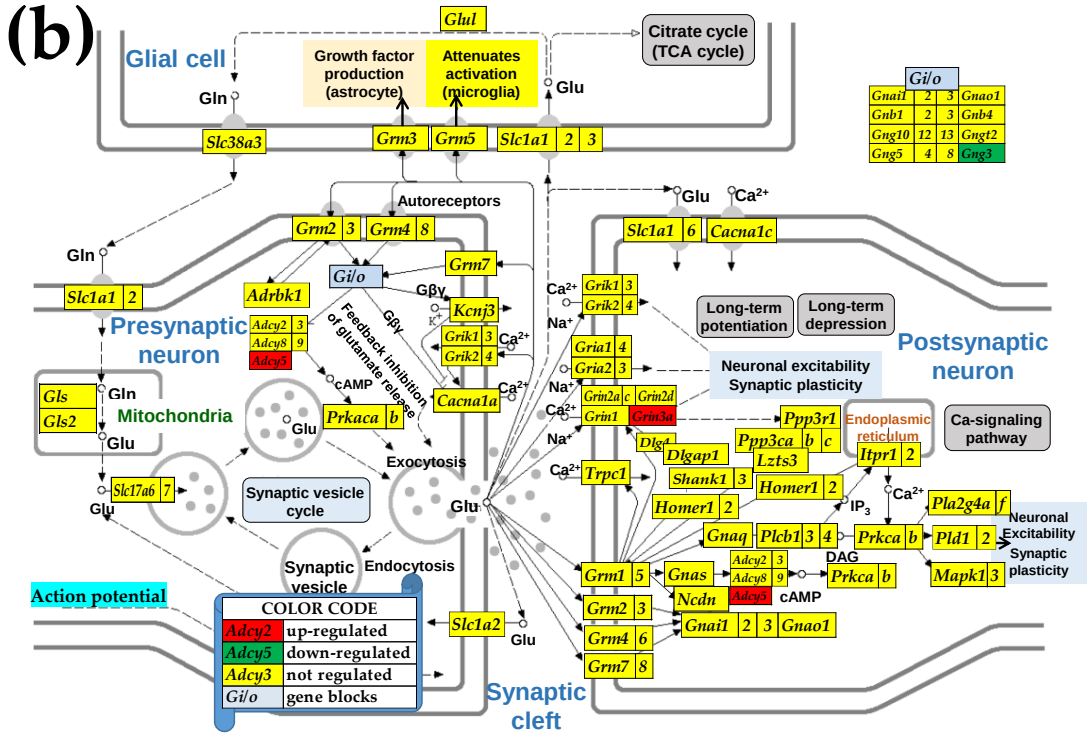

Figure 4. Significantly regulated genes in the KEGG-constructed Glutamatergic Synapse (GLU) pathway of the betamethasone-primed PVN of male (**a**) and female (**b**) rats following induction of the infantile spasms. Red/green background of the gene symbols indicate whether that gene was significantly up/down regulated by the induction of spasms in the betamethasone-primed animals, while yellow background indicates not significant regulation. Regulated genes: *Adcy2/5*, *Gls* (glutaminase (Gls), nuclear gene encoding mitochondrial protein), *Glul* (glutamate-ammonia ligase), *Gnai1* (guanine nucleotide binding protein (G protein), alpha inhibiting activity polypeptide 1), *Kcnj3* (potassium inwardly-rectifying channel, subfamily J, member 3), *Trpc1* (transient receptor potential cation channel, subfamily C, member 1).

3.6. Sex Differences Between the Significantly Regulated GABA Genes in the PVN by the Induction of Infantile Spasms in the Betamethasone-Primed Rats

Figure 5 presents the statistically significant ($p < 0.05$, absolute fold-change > CUT) regulations in the GABA functional pathway following induction of the infantile spasms in the betamethasone-primed state (BYS/BNS) of the PVN of male and female rats. Out of the 69 quantified GABA genes, four were up-regulated and two were down-regulated in males compared to one up-regulated and four down-regulated in females, with *Adcy5* being down-regulated in males but up-regulated in females.

 doi:10.20944/preprints202503.2046.v1

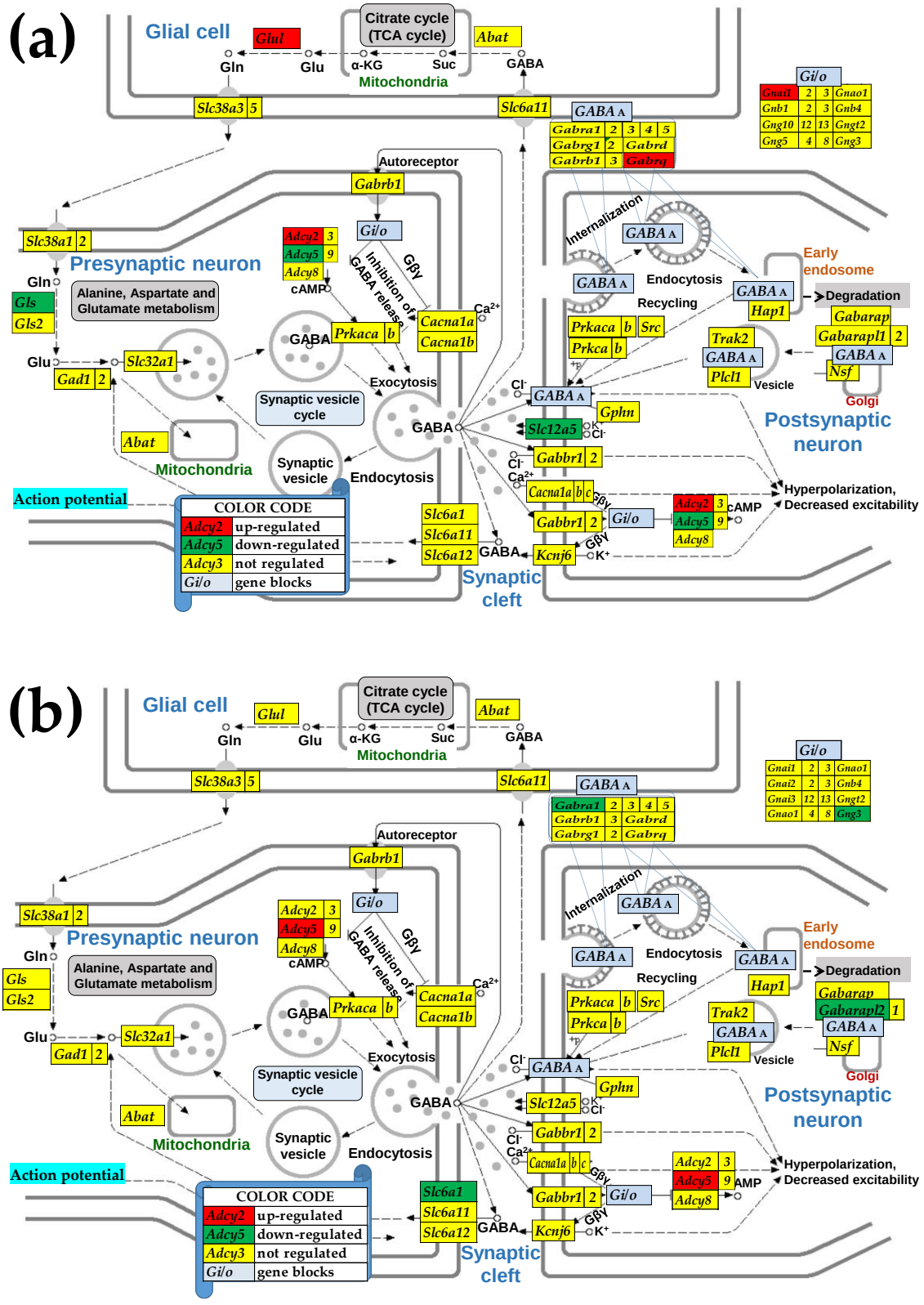

Figure 5. Significantly regulated genes in the KEGG-constructed GABA Synapse (GABA) pathway of the betamethasone-primed PVN of male (**a**) and female (**b**) rats following induction of the infantile spasms. Red/green background of the gene symbols indicates whether that gene was significantly up/down regulated by the induction of spasms in the betamethasone-primed animals, while yellow background indicates not significant regulation. Regulated genes: *Adcy2/5*, *Gabra1*, *Gabrq*, *Gabarapl2* (GABA(A) receptor-associated protein like 2), *Gls*, *Glul*, *Gnai1*, *Gng3*, *Slc12a5*, *Slc6a1* (solute carrier family 6 (neurotransmitter transporter), member 1).

 doi:10.20944/preprints202503.2046.v1

3.7. Sex Dichotomy of the Genes' Transcriptomic Networks

Figure 6 shows the significant differences between the two sexes in the correlated expressions of SVC genes. Panel (a) presents the SVC gene-pairs that are oppositely correlated in the two sexes, while, as shown in panels (b) and (c), several independently expressed gene pairs in one sex became significantly synergistically or antagonistically expressed in the other.

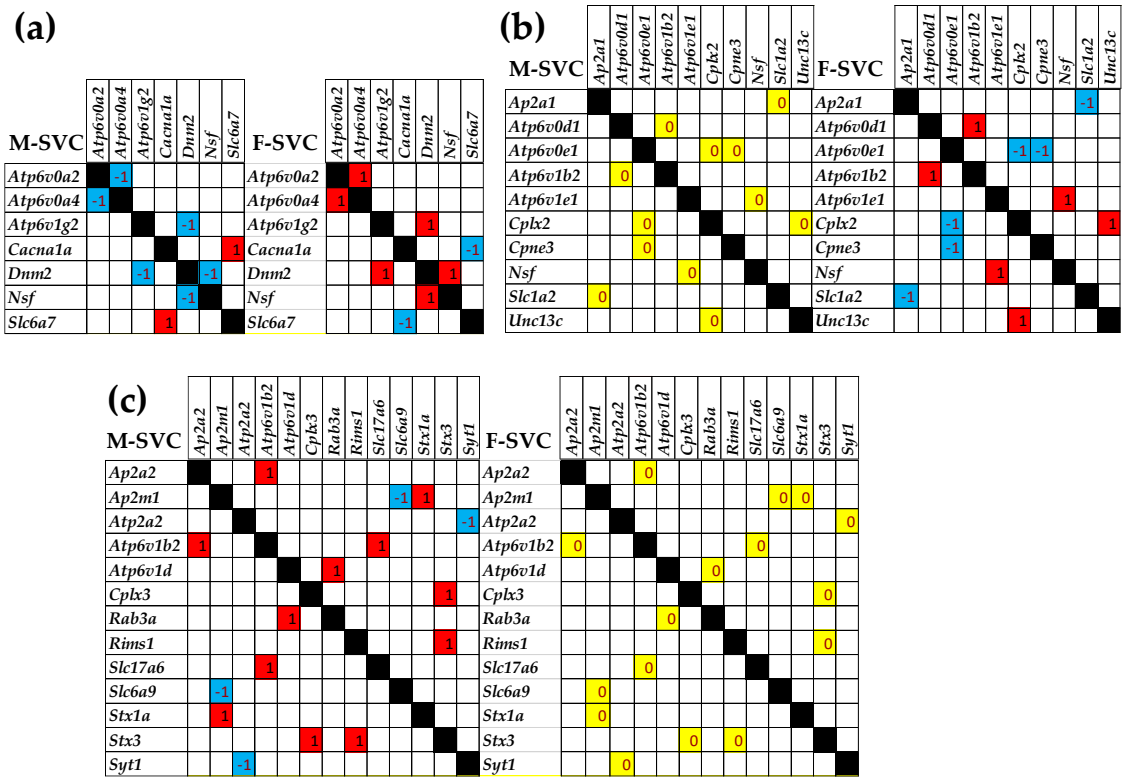

Figure 6. Significant sex dichotomy in the expression correlations among the SVC genes. (**a**) Gene pairs that switch their significant correlation from male to opposite in female. (**b**) Independently expressed gene-pairs in male which became significantly correlated in female. (**c**) Significantly correlated gene-pairs in male that are independently expressed in female. Interesting genes: *Ap2a1/m1* (adaptor-related protein complex 2, alpha 1/m1 subunit), *Atp2a2* (ATPase, Ca++ transporting, cardiac muscle, slow twitch 2), *Atpv0a2/4* (ATPase, H+ transporting, lysosomal V0 subunit A2/4), *Atp6v0d1/e1* (ATPase, H+ transporting, lysosomal V0 subunit D1/e1), *Atp6v1b2/e1/g2* (ATPase, H+ transporting, lysosomal V1 subunit B2/E1/G2), *Cacna1a* (calcium channel, voltage-dependent, P/Q type, alpha 1A subunit), *Cplx2* (complexin 2), *Cpne3* (copine III), *Dnm2* (dynamin 2), *Nsf* (N-ethylmaleimide-sensitive factor), *Rab3a* (RAB3A, member RAS oncogene family), *Slc1a2* (solute carrier family 1 (glial high affinity glutamate transporter)), *Unc13c* (unc-13 homolog C). .

Figure 7 shows the significant differences between the two sexes in the correlated expressions of GLU genes. Panel (a) presents the genes that are oppositely correlated in the two sexes. Thus, four antagonistically expressed gene pairs in male were switched to synergistically expressed in female (*Gls2 – Gng13*, *Gnao1 – Gria2*, *Gng5 – Itpr1*, *Grm2 – Slc38a2*), while two others (*Gnao1 – Gng8*, *Izts3 - Prkcg*) were switched from synergistically expressed in males to antagonistically expressed in females. Moreover, as shown in panels (b) and (c), several independently expressed gene pairs in one sex became significantly synergistically/antagonistically expressed in the other. All these differences indicate distinct molecular mechanisms involved in the glutamatergic synaptic transcription.

 doi:10.20944/preprints202503.2046.v1

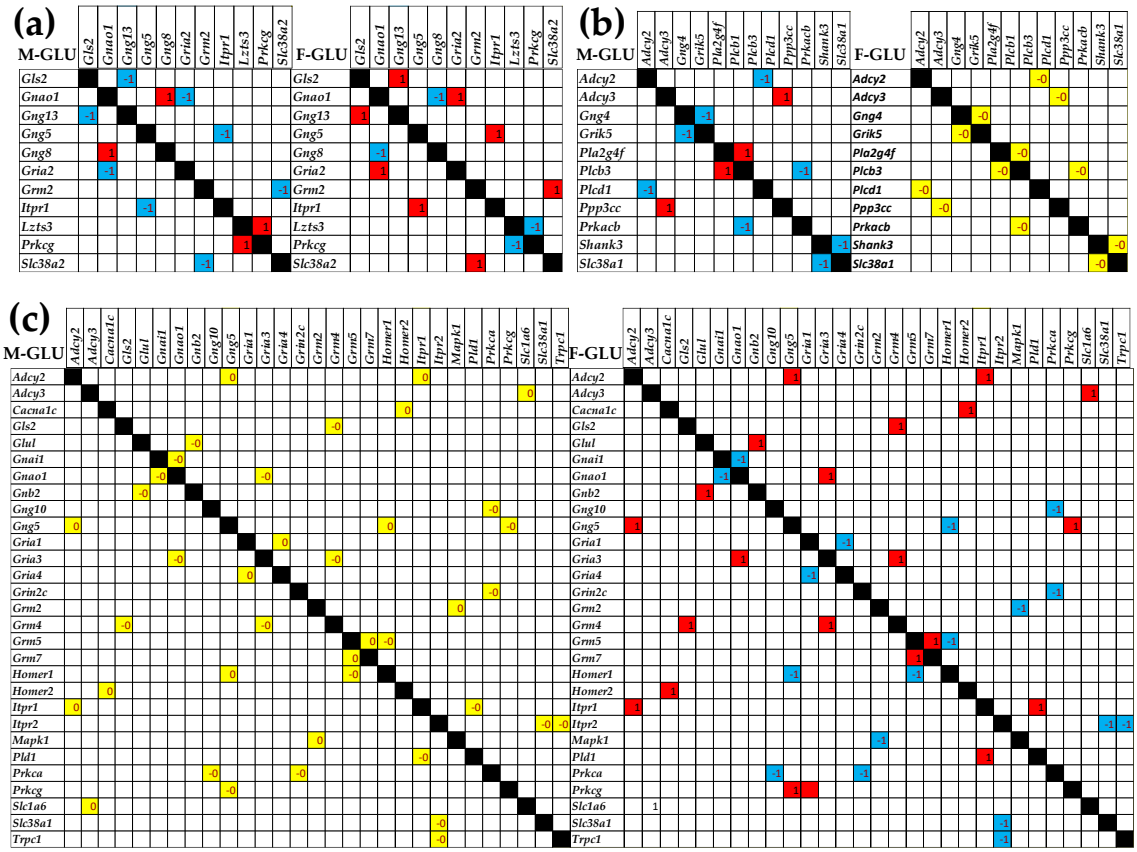

Figure 7. Significant sex dichotomy in the expression correlations among the GLU genes. (**a**) Gene pairs that switch their significant correlation in one sex to the opposite in the other. (**b**) Significantly synergistically and antagonistically correlated gene pairs in males that were independently expressed in females. (**c**) Significantly independently expressed genes in males that were significantly synergistically or antagonistically expressed in females.

3.8. Sex Dichotomy of the Genes' Hierarchy

Table 4 lists the most influential neurotransmission genes (higher GCH) and the Gene Master Regulators in all six groups of profiled samples. The relevant neurotransmission genes: *Gnb4*, *Gng10*, *Gng12* are part of all five synaptic pathways. *GCH* were computed using the software #GENE COMMANDING HEIGHT# [52]. Of note is the substantially lower GCH scores of the top neurotransmission genes with respect to the corresponding GMRs in the six groups: *Erg28* (40 vs 20 for *Pik3r2* in MSN), *Erap1* (70 vs 26 for *Abat* in FSN), *Tmem238* (162 vs 16 for *Gphn* in MBN), *Taf8* (38 vs 14 for *Grm8* in FBN), and *Tmem134* (78 vs 19 for *Mapk10* in MBY, respectively 78 vs *Homer1* in F-BYS).

 doi:10.20944/preprints202503.2046.v1

Table 4. The Gene Commanding Height (CGH) scores of the most influential neurotransmission genes compared to those of the Gene Master Regulators in all six groups of profiled samples.

	Most influential genes		Male			Female		
Gene	**Description**	**SYN**	**SNS**	**BNS**	**BYS**	**SNS**	**BNS**	**BYS**
Pik3r2	phosphoinositide-3-kinase, regulatory subunit 2	3	20	4	1	2	3	1
Gng12	guanine nucleotide binding protein (G protein), gamma 12	12345	8	2	8	5	1	8
Ppp1ca	protein phosphatase 1, catalytic subunit, alpha isozyme	4	7	9	4	2	6	4
Ppp2r1a	protein phosphatase 2, regulatory subunit A, alpha	4	7	3	2	3	1	2
Calml4	calmodulin-like 4	4	6	2	3	2	1	3
Abat	4-aminobutyrate aminotransferase	2	3	4	5	26	6	5
Pld1	phospholipase D1	1	1	1	2	17	1	2
Slc6a7	solute carrier family 6 (neurotransmitter transporter), member 7	0	4	1	4	11	1	4
Gabra1	gamma-aminobutyric acid (GABA) A receptor, alpha 1	2	1	2	4	8	2	4
Homer1	homer homolog 1	1	1	2	13	8	2	13
Gphn	gephyrin	2	3	16	0	3	2	0
Ap2a2	adaptor-related protein complex 2, alpha 2 subunit	0	1	16	3	2	2	3
Creb3l1	cAMP responsive element binding protein 3-like 1	34	1	14	4	3	1	4
Gng10	guanine nucleotide binding protein (G protein), gamma 10	12345	2	11	4	2	3	4
Gabbr1	gamma-aminobutyric acid (GABA) B receptor 1	2	1	10	5	5	2	5
Grm8	glutamate receptor, metabotropic 8	1	2	1	5	3	14	5
Cpne3	copine III	0	2	2	2	1	14	2
Atp6v1h	ATPase, H+ transporting, lysosomal V1 subunit H	0	4	3	6	2	12	6
Atp6v0e1	ATPase, H+ transporting, lysosomal, V0 subunit e1	0	3	1	1	3	12	1
Gabarapl2	GABA(A) receptor-associated protein like 2	2	3	8	7	1	10	7
Mapk10	mitogen activated protein kinase 10	4	2	6	19	1	1	19
Homer1	homer homolog 1	1	1	2	13	8	2	13
Th	tyrosine hydroxylase	4	1	1	11	2	1	11
Gnb4	guanine nucleotide binding protein (G protein), beta polypeptide 4	12345	3	5	10	6	1	10
Glul	glutamate-ammonia ligase	12	1	1	10	3	5	10
Mapk10	mitogen activated protein kinase 10	4	2	6	19	1	1	19
Homer1	homer homolog 1	1	1	2	13	8	2	13
Th	tyrosine hydroxylase	4	1	1	11	2	1	11
Gnb4	guanine nucleotide binding protein (G protein), beta polypeptide 4	12345	3	5	10	6	1	10
Glul	glutamate-ammonia ligase	12	1	1	10	3	5	10
Erg28	ergosterol biosynthesis 28 homolog		**40**	6	1	3	7	1
Erap1	endoplasmic reticulum aminopeptidase 1		2	2	2	**70**	2	2
Tmem238	transmembrane protein 238		4	**162**	3	3	4	3
Taf8	TAF8 RNA polymerase II, TATA box binding protein (TBP)-associated factor		1	1	3	5	**38**	3
Tmem134	transmembrane protein 134		2	7	**78**	5	2	78

4. Discussion

While certian sex-specific prevalence of IESS in boys were discovered in large cohort studies [22] and we also saw trends to increased susceptibility in males, this never reached statistical significance in our relatively small experimental cohorts (<20 per sex group) on an ISa rat model. However, the very sensitive and unbiased transcriptomic analyses were able to provide a glimse on the significant sex dichotomy in the genomic molecular machinery.

The analyses of six neurotransmission pathways in the PVNs of male and female rats at P16 revealed substantial transcriptomic differences between the two sexes, that persists also in the betamethasone prenatally primed pups without triggered spasms. Beyond traditional gene expression studies that are limited to quantifying the expression profile, our approach incorporates two additional independent measures of the individual genes: control of transcripts' abundances and inter-coordination of their expression. Together, the three independent measures provide the most comprehenssive characterization of the two sexes PVN transcriptomic topologies and their differential remodeling in infantile spasms.

Although the tissue pieces were very small, they were still heterocellular, that is one major limitation of this study. In the worst scenario, the non-significant change of gene when comparing different conditions for the same sex or different sexes for the same condition, might result from up-regulation in a particular phenotype and down-regulation in another. However, taking a particular type of cells from their natural environment would have a larger effect on the transcriptome, as we proved by profiling cortical astrocytes and precursor oligodendrocytes when co-cultured and cultured separately [55–57].

We found (Table 1) little sex differences between the expression levels of the top neurotransmission genes. For instance, the active regulator of intracellular Ca^{2+} release *Caly* has the

 doi:10.20944/preprints202503.2046.v1

largest expression level among all neurotransmission genes in the PVNs of both sexes in all three investigated conditions. Abundance of *Cali* transcripts was between 126 and 195 times larger than the expression level of the median gene in the respective group, close enough to *Cst3* and *Rpl41*, the top expressed genes in the entire transcriptome. *Cali*, localized in the neuron dendritic spines, is related to D1 dopaminergic transmission and schizophrenia [31,32]. However, expression of *Caly* (Table 2) was less controlled than the median gene in all groups: REC = -0.98 in MSN, -0.41 in FSN, -1.26 in MBN, -0.90 in FBN, -0.85 in MBY, and -0.69 in FBY, indicating remarkable flexibility.

As seen in Table 2, the most controlled neurotransmission genes are: *Pik3r2* and *Abat* in the two SN groups, *Pik3r5* and *Grm8* in BNSs, and *Th* and *Trpc1* in BYSs. Interestingly, mutation of *Pik3R2* was associated with familial temporal lobe epilepsy [58] and its overexpression may reduce cell viability and boost autophagy and apoptosis. [59]. GABA transaminase deficiency caused by mutation of *Abat* leads to neonatal epilepsy [60], while activation through the FOXA2/ABAT/GABA axis mediate development of brain metastasis in lung cancer [61]. Therefore, the high control of these two genes in the normal condition (SN) prevents neurotransmission alterations associated with IEES in the corresponding sex.

Moreover (see Supplementary Table S2a for the M/F ratios of RCS), neurogenes like: *Mapk10* in SN, *Pik3r5* (BN), and *Th* (BY) are strictly controlled in males but allowed to fluctuate in females in the corresponding conditions. In contrast, genes like: *Abat* and *Gabbr1* in SN and *Trpc1* (BY) are flexibly expressed in males but strictly controlled in females in the corresponding conditions. Both *Mapk10* and *Gabbr1* are considered as potential targets for vascular dementia treatment [62,63].The differences are even larger for the top controlled genes in each condition, with *Erg28, Tmem238* and *Oxsr1* very strictly controlled in males but much less controlled in females, while the opposite is observed for *Erap1, Cul7* and *Tac2.* All these differences point to distinct homeostatic mechanisms that control the transcripts' abundances.

The effect of IEES triggering in betamethasone primed rats (BY condition) has distinct sex-dependent effects on genes' RCSs (Supplementary Table S2b). While the RCSs of *Pik3r2* is increased by IEES in males (by 6.49x) with little effect on females, that of *Gnal* is increased in females (by 8.84x). *Gnal* larger effects on female than on male dystonia was recently documented in a population study [64].

There are also substantial sex differences among the most flexibly expressed neuro-transmission genes (Table 3) in all three conditions: *Calml1* vs. *Mapk10* in SN, *Drd2* vs *Creb3* in BN, and *Clock* vs *Grin1* in BY. Interestingly, all the top flexible genes are included in the dopaminergic synapse pathway. Although several other reports discussed sex-differences in the expressions of neurotransmission genes and their encoded proteins (e.g. [65–69]), we here report for the first time the sex dichotomy in gene expression control.

Th, a rate-limiting enzyme (tyrosine hydroxylase) in dopamine, epinephrine, and norepinephrine biosynthesis [70] has a spectacular (by 44.51x) RCS increase in IESS with respect to the healthy counterpart in males (Supplementary Table S3), that is also 14.58x larger than in females BYS. Therefore, we consider that *Th* might be a potential gene therapy target for future research for a male with IESS, but not for a female with IESS.

In contrast, the control strength of *Creb3* in females decreased significantly (by 8.68x) in both BN and BY conditions (Supplementary Table S3). *Creb3* protein tethers chromatin to the cell inner nuclear membrane and preventing karyoptosis, a type of cell death caused by DNA release into cytosol [71]. Therefore, the high expression flexibility of the encoding gene makes both cholinergic and dopaminergic transmission more adaptable to prenatal corticosteroids, even in the absence of IS.

Figure 2a shows a higher synaptic vesicle acidification following endocytosis but a lower neurotransmission uptake in male versus female PVN. Apparently, these differences indicate that in males, there is a higher efficiency in recycling the synaptic vesicles, yet decreased release of neurotransmitters compared to females. However, as demonstrated in Figure 3ab, IESS induction does not cause an overall imbalance of the synaptic vesicle cycle in either sex. Interestingly, reports by others demonstrated that some factors such as exposure to diazepam [72] or maternal immune

 doi:10.20944/preprints202503.2046.v1

activation [73] affect the synaptic vesicle cycle pathway. We further found substantial differences between the significantly regulated genes by IESS in males (Figure 2a) and in females (Figure 2b). For instance, while in males, the ATPase *Atp2a2* (a.ka. *Serca2*), involved in actvely pumping Ca^{2+} from the cytosol into the endoplasmic reticulum and a candidate gene for IESS [74] is down-regulated, it is up-regulated in females.

Figure 2b indicates lower glutamateric transmission in control saline-injected (i.e. SN) male compared to the female PVN, caused by the underexpression of *Grik1* and Slc1a2 in the presynaptic neuron. The higher expression of *Grik1* in women relative to that in men was also detected in patients with depression [75]. Through the underexpression of *Gabra4*, *Gabrd*, and *Gabrdg1*, Figure 2c confirms the report [76] of male rats lagging behind females in the development of the ionotropic of GABA-A receptors. Underexpression of the G-proteins *Gnb4* and *Gng5* in males with respect to their female counterparts was common to all five investigated synapse pathways (Figures 2b-2f). These G-proteins are involved in the presynaptic inhibition, dimishing the release of glutamate, GABA and Ach release in the synaptic cleft [77,78]. However, the effect of the reduced expression of the G-proteins is compensated by the increased expression of the inositol 1,4,5-trisphosphate receptors *Itpr1* and *Itpr2* (*Itpr3* was not quantified). Activation these receptors releases Ca^{2+} (that controls almost all important cellular processes [79]) from the intracellular IP_3-sensitive storages [80].

The differences between the two sexes appear also in the regulomes of SVC (Figure 3), GLU (Figure 4) and GABA (Figure 5) pathways after induction of IS. For instance, the presynaptic regulatory protein *Cplx2* (complexin 2), whose variants affect cognition in schizophrenic patients [81], is down-regulated in males (Figure 3a) but upregulated in females (Figure 3b). Expression of several genes (e.g. *Kcnj3, Trpc1*) were not affected in one sex (female) but significantly regulated in the other. These findings suggest that dissimilar pathological processes affected the neurotransmission in the two sexes. Among others, our result explains why suppression of the potassium channel encoded by *Kcnj3* impairs prelimbic cortical function in male, but not female, mice [82].

Figure 6 presents the spectacular differences between the male and female statistically significant SVC pathway transcriptome network. Thus, three antagonistically expressed gene pairs in males (*Atp6v0a2–Atp6v0a4*, *Atp6v1g2–Dnm2*, *Dnm2-Nsf*) are switched to synergistically expressed pairs in females, while the pair *Cacna1a–Slc6a7* was switched from synergistically expressed in males to antagonistically expressed in females (Figure 6a). Moreover, six independently expressed gene-pairs in males are significantly synergistically or antagonistically correlated in females (Figure 6b), and eight synergistically or antagonistically expressed in males are independently expressed in females (Figure 6c).

Given the roles of v-ATPase a subunits in phagocytosis, endocytosis and autophagy [83], it would be interesting to study the functional consequences of the opposite expression coordinations of *Atp6v0a2* and *Atp6v0a4* in the two sexes. Of note is the sex discrepancy in the expression correlation of the dynamin *Dnm2*, responsible for vesicle recovery after releasing the neurotransmitters into the synaptic cleft with the v-ATPase *Atp6v1g2* involved in vesicle accidification needed for neurotransmitter uptake. Also surprising is the antagonistic expression of *Nsf* (that removes the cis-SNARE complex [84]) and *Dnm2* in males while they are supposed to stimulate each-other expression (as it happens in female).

Likewise, we found substantial sex differences in the transcriptomic networks of GLU pathway. Thus, the antagonistically expressed pairs in males: *Gng13-Gls2, Gria2-Gnao1, Itpr1-Gng5, Slc38a2-Grm2* are synergistically expressed in females, while the synergisti]cally expressed pairs in males: *Gng8-Gnao1, Prkcg-Lzts3* are antagonistically expressed in females (Figure 6a). In addition, six significantly correlated gene-pairs in males are independently expressed in females and 20 (*sic!*) independently expressed pairs in males are significantly correlated in females. The opposite expression correlations of *Gng13* with *Gls2* in the two sexes suggest opposite relationship between mitophagy and feedback inhibition of glutamate release. Such coordination might have consequences on the epilepsy occurance [85], where *Gls2* is down-regulated (as we also found, Figure 4a).

 doi:10.20944/preprints202503.2046.v1

All these transcriptomic network differences indicate distinct molecular mechanisms responsible for the formation of synaptic vesicles, release of neurotransmitters, and response by the post-synaptic neuron in the PVNs of the two sexes. The neurotransmission differences are most likely responsible for different brain circuitries in males and females (e.g. [86–88])

Interestingly we observed that the genes involved in neurotransmission are not among the most influential in both male and female rats subjected to each of the three conditions. Yest, the most prominent genes in the IESS condition, *Grm8* (male) and *Mapk10* (female) have documented implications in epilepsy (e.g. [89–91]). However, present study pinpoints *Tmem134,* a protein located in the perinuclear region of the cytoplasm, involved in RNA splicing [92] and associated with obesity [93], as the best target for the gene therapy of IS in rats of both sexes. In previous reports, we assumed and verified [52,94] that manipulation of genes with higher *GCH* has larger consequences on the transcriptome, the top gene, named Gene Master Regulator (GMR) being the most influential, whose silence might be lethal for the cell.

5. Conclusions

Our transcriptomic analysis of six neurotransmission pathways in the PVN of P16 12 male and 12 female rats revealed substantial sex differences, persisting even in prenatally betamethasone-primed pups, regardless of NMDA triggering of IESS. By integrating expression level, transcript abundance control, and expression inter-coordination, we provide a comprehensive molecular characterization of these differences. Nonetheless, because transcripts abundances and protein content are not proportional [95,96] (gene transcription is triggered by the necessity to keep a certain level of protein), our results cannot be automatically translated into sex-dependent proteome topology and remodeling by IESS.

Sex-specific transcriptomic shifts in synaptic vesicle cycling, glutamatergic, and GABAergic pathways suggest distinct pathological mechanisms, influenced by the sex hormones [97–99]. We found that gene co-expression patterns differed, highlighting fundamental sex-dependent synaptic organization that determine brain cirucuits (e.g. [101,102]). This study extends our previous findings of sex transcriptomic dichotomy in regions of the brain [8–10], heart [103,104], and kidneys [105].

Finally, in our rat model, *Tmem134* (encoding cytosolic and membrane protein likely involved in the cytokine pathway [33]) emerged as the most influential gene for IESS pathology in both sexes. Nevertheless, the dominance of *Tmem134* is surprising and deserves to be tested in further experiments on the same IEES rat model.

Supplementary Materials: The following supporting information can be downloaded at the website of this paper posted on Preprints.org. **Table S1: Expression ratios (negative for down-regulation) between the two sexes in the three conditions.** Path = 0 (SVC), 1 (GLU), 2 (GAB), 3 (CHO), 4 (DOP), 5 (SER). **Table S2a: Ratios of the Relative Strength Controls (negative for down-regulation) between the two sexes in the three** conditions**.** Path = 0 (SVC), 1 (GLU), 2 (GAB), 3 (CHO), 4 (DOP), 5 (SER). Red/green background indicates large differences. **Table S2b: Ratios of the Relative Strength Controls (negative for down-regulation) between BY and SN in the two sexes in the three conditions.** Path = 0 (SVC), 1 (GLU), 2 (GAB), 3 (CHO), 4 (DOP), 5 (SER). Red/green background indicates large differences. **Table S3: Ratios of the Relative Strength Controls (negative for down-regulation) between the two sexes in the three conditions.** Path = 0 (SVC), 1 (GLU), 2 (GAB), 3 (CHO), 4 (DOP), 5 (SER). Red/green background indicates large differences. **Table S4: Ratios of the Relative Strength Controls (negative for down-regulation) between the BY and SN in the two sexes.** Path = 0 (SVC), 1 (GLU), 2 (GAB), 3 (CHO), 4 (DOP), 5 (SER). Red/green background indicates large differences.

Author Contributions: Conceptualization, D.A.I. and L.V.; methodology, D.A.I., T.C., C.-R.C.; software, D.A.I.; validation, S.I., D.A.I. and T.C. C.-R.C., K.V., J.V., L.V.; formal analysis, D.A.I.; investigation, S.I., L.V., J.V., K.V; resources, D.A.I. and L.V.; data curation, D.A.I.; writing—original draft preparation, D.A.I., J.V., T.C., C.-R.C., K.V., L.V.; writing—review and editing, D.A.I.; J.V., T.C., C.-R.C., K.V., L.V.; visualization, S.I.; supervision, D.A.I., L.V.; project administration, D.A.I.; funding acquisition, L.V. All authors have read and agreed to the published version of the manuscript.

 doi:10.20944/preprints202503.2046.v1

Funding: Supported by the NIH awards RC4 NS072966, R21 NS118337, by CURE Epilepsy Infantile Spasms Consortium Award, and by Graduate School of Biomedical Sciences at the New York Medical College.

Institutional Review Board Statement: The animal study protocol was approved by the IACUC of New York College of Medicine, #52-1-0913 approved on 9/25/2013 for 3 years.

Data Availability Statement: The wet protocol and the microarray raw data were deposited in the publicly accessible Gene Ex-pression Omnibus (https://www.ncbi.nlm.nih.gov/geo/query) as: GSE123721, GSE124613, 128091.

References

1. Synaptic vesicle cycle. Available on line at: https://www.genome.jp/kegg-bin/show_pathway?rno04721. Accessed on: 12/12/2024..
2. Glutamatergic synapse. Available at https://www.genome.jp/pathway/rno04724. Access on: 12/12/2024.
3. GABAergic synapse. Available at: https://www.genome.jp/kegg-bin/show_pathway?rno04727. Accessed on: 12/12/2024.
4. Cholinergic synapse. Available at: https://www.genome.jp/kegg-bin/show_pathway?rno04725. Accessed on: 12/12/2024.
5. Dopaminergic synapse. Available at: https://www.genome.jp/kegg-bin/show_pathway?rno04728. Accessed on: 12/12/2024.
6. Serotonergic synapse. Available at: https://www.genome.jp/kegg-bin/show_pathway?rno04726. Accessed on: 12/12/2024.
7. Velíšek, L.; Jehle, K.; Asche, S.; Velíšková, J. Model of infantile spasms induced by N-methyl-D-aspartic acid in prenatally impaired brain. *Ann Neurol* **2007**, *61*, 109-119.
8. Iacobas, D.A.; Iacobas, S.; Chachua, T.; Goletiani, C.; Sidyelyeva, G.; Veliskova, J.; Velisek, L. Prenatal corticosteroids modify glutamatergic and GABAergic synapse genomic fabric: insights from a novel animal model of infantile spasms. *J Neuroendocrinol* **2013**, *25*, 964-979, doi:10.1111/jne.12061.
9. Iacobas, D.A.; Chachua, T.; Iacobas, S.; Benson, M.J.; Borges, K.; Veliskova, J.; Velisek, L. ACTH and PMX53 recover synaptic transcriptome alterations in a rat model of infantile spasms. *Sci Rep* **2018**, *8*, 5722, doi:10.1038/s41598-018-24013-x.
10. Iacobas, D.A.; Velisek, L. Regeneration of neurotransmission transcriptome in a model of epileptic encephalopathy after antiinflammatory treatment. *Neural Regen Res* **2018**, *13*, 1715-1718, doi:10.4103/1673-5374.238607.
11. Hrachovy, R.A. West's syndrome (infantile spasms). Clinical description and diagnosis. *Advances in experimental medicine and biology* **2002**, *497*, 33-50.
12. Dulac, O.; Soufflet, C.; Chiron, C.; Kaminska, A. What is West syndrome? *Int Rev Neurobiol* **2002**, *49*, 1-22.
13. Hrachovy, R.A.; Frost, J.D., Jr. Infantile spasms. *Handbook of clinical neurology* **2013**, *111*, 611-618, doi:10.1016/B978-0-444-52891-9.00063-4.
14. Pavone, P.; Striano, P.; Falsaperla, R.; Pavone, L.; Ruggieri, M. Infantile spasms syndrome, West syndrome and related phenotypes: what we know in 2013. *Brain Dev* **2014**, *36*, 739-751, doi:10.1016/j.braindev.2013.10.008.
15. Mackay, M.T.; Weiss, S.K.; Adams-Webber, T.; Ashwal, S.; Stephens, D.; Ballaban-Gill, K.; Baram, T.Z.; Duchowny, M.; Hirtz, D.; Pellock, J.M.; et al. Practice parameter: medical treatment of infantile spasms: report of the American Academy of Neurology and the Child Neurology Society. *Neurology* **2004**, *62*, 1668-1681.
16. Go, C.Y.; Mackay, M.T.; Weiss, S.K.; Stephens, D.; Adams-Webber, T.; Ashwal, S.; Snead, O.C., 3rd; Child Neurology, S.; American Academy of, N. Evidence-based guideline update: medical treatment of infantile spasms. Report of the Guideline Development Subcommittee of the American Academy of Neurology and the Practice Committee of the Child Neurology Society. *Neurology* **2012**, *78*, 1974-1980, doi:10.1212/WNL.0b013e318259e2cf.
17. Riikonen, R. The latest on infantile spasms. *Curr Opin Neurol* **2005**, *18*, 91-95, doi:00019052-200504000-00003 [pii].

 doi:10.20944/preprints202503.2046.v1

18. Lux, A.L.; Edwards, S.W.; Hancock, E.; Johnson, A.L.; Kennedy, C.R.; Newton, R.W.; O'Callaghan, F.J.; Verity, C.M.; Osborne, J.P. The United Kingdom Infantile Spasms Study (UKISS) comparing hormone treatment with vigabatrin on developmental and epilepsy outcomes to age 14 months: a multicentre randomised trial. *Lancet Neurol* **2005**, *4*, 712-717.
19. Riikonen, R. Long-term outcome of patients with West syndrome. *Brain Dev* **2001**, *23*, 683-687, doi:S0387760401003072 [pii].
20. Luthvigsson, P.; Olafsson, E.; Sigurthardottir, S.; Hauser, W.A. Epidemiologic features of infantile spasms in Iceland. *Epilepsia* **1994**, *35*, 802-805.
21. Harini, C.; Nagarajan, E.; Bergin, A.M.; Pearl, P.; Loddenkemper, T.; Takeoka, M.; Morrison, P.F.; Coulter, D.; Harappanahally, G.; Marti, C.; et al. Mortality in infantile spasms: A hospital-based study. *Epilepsia* **2020**, *61*, 702-713, doi:10.1111/epi.16468.
22. Hancock, E.C.; Osborne, J.P.; Edwards, S.W. Treatment of infantile spasms. *Cochrane Database Syst Rev* **2013**, CD001770, doi:10.1002/14651858.CD001770.pub3.
23. Chachua, T.; Yum, M.-S.; Velíšková, J.; Velíšek, L. Validation of the rat model of cryptogenic infantile spasms. *Epilepsia* **2011**, *52*, 1666-1677.
24. Mareš, P.; Velíšek, L. N-methyl-D-aspartate (NMDA)-induced seizures in developing rats. *Brain Res Dev Brain Res* **1992**, *65*, 185-189.
25. Yum, M.S.; Chachua, T.; Velíšková, J.; Velíšek, L. Prenatal stress promotes development of spasms in infant rats. *Epilepsia* **2012**, *53*, e46-49, doi:10.1111/j.1528-1167.2011.03357.x.
26. Tsuji, M.; Takahashi, Y.; Watabe, A.M.; Kato, F. Enhanced long-term potentiation in mature rats in a model of epileptic spasms with betamethasone-priming and postnatal N-methyl-d-aspartate administration. *Epilepsia* **2016**, *57*, 495-505, doi:10.1111/epi.13315.
27. Baek, H.; Yi, M.H.; Pandit, S.; Park, J.B.; Kwon, H.H.; Zhang, E.; Kim, S.; Shin, N.; Kim, E.; Lee, Y.H.; et al. Altered expression of KCC2 in GABAergic interneuron contributes prenatal stress-induced epileptic spasms in infant rat. *Neurochemistry international* **2016**, *97*, 57-64, doi:10.1016/j.neuint.2016.05.006.
28. Janicot, R.; Shao, L.R.; Stafstrom, C.E. 2-deoxyglucose and beta-hydroxybutyrate fail to attenuate seizures in the betamethasone-NMDA model of infantile spasms. *Epilepsia Open* **2022**, *7*, 181-186, doi:10.1002/epi4.12561.
29. Savic, B.; Murphy, D.; Japundzic-Zigon, N. The Paraventricular Nucleus of the Hypothalamus in Control of Blood Pressure and Blood Pressure Variability. *Front Physiol* **2022**, *13*, 858941, doi:10.3389/fphys.2022.858941.
30. Velíšková, J. Sex matters in epilepsy. In *Developmental Epilepsy: From Clinical Medicine to Neurobiological Mechanisms*, Stafstrom, C.E., Velíšek, L. , Ed.; World Scientific Publishing: Singapore, 2019; pp. 387-405.
31. Koh, P.O.; Bergson, C.; Undie, A.S.; Goldman-Rakic, P.S.; Lidow, M.S. Up-regulation of the D1 dopamine receptor-interacting protein, calcyon, in patients with schizophrenia. *Arch Gen Psychiatry* **2003**, *60*, 311-319, doi:10.1001/archpsyc.60.3.311.
32. Ha, C.M.; Park, D.; Han, J.K.; Jang, J.I.; Park, J.Y.; Hwang, E.M.; Seok, H.; Chang, S. Calcyon forms a novel ternary complex with dopamine D1 receptor through PSD-95 protein and plays a role in dopamine receptor internalization. *J Biol Chem* **2012**, *287*, 31813-31822, doi:10.1074/jbc.M112.370601.
33. Tian, Y.; Huang, W.; Yang, J.; Wen, Z.; Geng, Y.; Zhao, C.; Zhang, H.; Wang, Y. Systematic identification of hepatitis E virus ORF2 interactome reveals that TMEM134 engages in ORF2-mediated NF-kappaB pathway. *Virus Res* **2017**, *228*, 102-108, doi:10.1016/j.virusres.2016.11.027.
34. Gold, M.S.; Blum, K.; Oscar-Berman, M.; Braverman, E.R. Low dopamine function in attention deficit/hyperactivity disorder: should genotyping signify early diagnosis in children? *Postgrad Med* **2014**, *126*, 153-177, doi:10.3810/pgm.2014.01.2735.
35. Puig, M.V.; Gulledge, A.T. Serotonin and prefrontal cortex function: neurons, networks, and circuits. *Mol Neurobiol* **2011**, *44*, 449-464, doi:10.1007/s12035-011-8214-0.
36. Lei, S. Serotonergic modulation of Neural activities in the entorhinal cortex. *Int J Physiol Pathophysiol Pharmacol* **2012**, *4*, 201-210.

 doi:10.20944/preprints202503.2046.v1

37. Seyedabadi, M.; Fakhfouri, G.; Ramezani, V.; Mehr, S.E.; Rahimian, R. The role of serotonin in memory: interactions with neurotransmitters and downstream signaling. *Exp Brain Res* **2014**, *232*, 723-738, doi:10.1007/s00221-013-3818-4.
38. Bakker, J. The role of steroid hormones in the sexual differentiation of the human brain. *J Neuroendocrinol* **2022**, *34*, e13050, doi:10.1111/jne.13050.
39. Cutia, C.A.; Christian-Hinman, C.A. Mechanisms linking neurological disorders with reproductive endocrine dysfunction: Insights from epilepsy research. *Front Neuroendocrinol* **2023**, *71*, 101084, doi:10.1016/j.yfrne.2023.101084.
40. Akman, O.; Moshe, S.L.; Galanopoulou, A.S. Sex-specific consequences of early life seizures. *Neurobiol Dis* **2014**, *72 Pt B*, 153-166, doi:10.1016/j.nbd.2014.05.021.
41. Iacobas, S.; Iacobas, D.A. . Analyzing the Cytoskeletal Transcriptome: Sex Differences in Rat Hypothalamus. In: Dermietzel, R. (eds) The Cytoskeleton. *Neuromethods* **2013**, *79*.
42. Velíšková, J.; Iacobas, D.; Iacobas, S.; Sidyelyeva, G.; Chachua, T.; Velíšek, L. Oestradiol Regulates Neuropeptide Y Release and Gene Coupling with the GABAergic and Glutamatergic Synapses in the Adult Female Rat Dentate Gyrus. *J Neuroendocrinol* **2015**, *27*, 911-920, doi:10.1111/jne.12332.
43. Bakker, J. The Sexual Differentiation of the Human Brain: Role of Sex Hormones Versus Sex Chromosomes. *Curr Top Behav Neurosci* **2019**, *43*, 45-67, doi:10.1007/7854_2018_70.
44. Sex differences in the synaptic genomic fabrics of the rat hypothalamic paraventricular node. Available online at: https://www.ncbi.nlm.nih.gov/geo/query/acc.cgi?acc=GSE123721. Accessed on 01/04/2025..
45. Prenatal betamethasone remodels the genomic fabrics of the synaptic transmission in the rat hypothalamic paraventricular nucleus. Available on line at: https://www.ncbi.nlm.nih.gov/geo/query/acc.cgi?acc=GSE124613. Accessed on 01/04/2025.
46. Remodeling of synaptic transmission genomic fabrics in the hypothalamic paraventricular nucleus of a rat model of autism. Available online at: https://www.ncbi.nlm.nih.gov/geo/query/acc.cgi?acc=GSE128091. Accessed on: 01/04/2025
47. Iacobas, D.A. The Genomic Fabric Perspective on the Transcriptome Between Universal Quantifiers and Personalized Genomic Medicine. *Biol Theory* **2016**, *11*, 123-137, doi:https://doi.org/10.1007/s13752-016-0245-3.
48. Iacobas, D.A.; Iacobas, S.; Lee, P.R.; Cohen, J.E.; Fields, R.D. Coordinated Activity of Transcriptional Networks Responding to the Pattern of Action Potential Firing in Neurons. *Genes (Basel)* **2019**, *10*, doi:10.3390/genes10100754.
49. Bicknell, R.J. Sex-steroid actions on neurotransmission. *Curr Opin Neurol*. **1998** 11(6):667-71. doi: 10.1097/00019052-199812000-00010.
50. Foster, T.C.; Kumar, A. Sex, senescence, senolytics, and cognition. *Front Aging Neurosci*. **2025** 4;17:1555872. doi: 10.3389/fnagi.2025.1555872.
51. Sinclair, D.; Purves-Tyson, T.D.; Allen, K.M.; Weickert, C.S. Impacts of stress and sex hormones on dopamine neurotransmission in the adolescent brain. *Psychopharmacology (Berl)*. **2014**; 231(8):1581-99. doi: 10.1007/s00213-013-3415-z.
52. Iacobas, S.; Ede, N.; Iacobas, D.A. The Gene Master Regulators (GMR) Approach Provides Legitimate Targets for Personalized, Time-Sensitive Cancer Gene Therapy. *Genes (Basel)* **2019**, *10*, doi:10.3390/genes10080560.
53. Krishna, S.; Cheng, B.; Sharma, D.R.; Yadav, S.; Stempinski, E.S.; Mamtani, S.; Shah, E.; Deo, A.; Acherjee, T.; Thomas, T.; et al. PPAR-gamma activation enhances myelination and neurological recovery in premature rabbits with intraventricular hemorrhage. *Proc Natl Acad Sci U S A* **2021**, *118*, doi:10.1073/pnas.2103084118.
54. Kanehisa, M. The KEGG database. *Novartis Found Symp*. **2002**;247:91-101; discussion 101-3, 119-28, 244-52.
55. Iacobas, S.; Iacobas, D.A. Astrocyte proximity modulates the myelination gene fabric of oligodendrocytes. *Neuron Glia Biol*. **2010**; 6(3):157-69. doi: 10.1017/S1740925X10000220.
56. Iacobas, S.; Thomas, N.M.; Iacobas, D.A. Plasticity of the myelination genomic fabric. Mol Genet Genomics. **2012**; 287(3):237-46. doi: 10.1007/s00438-012-0673-0.

 doi:10.20944/preprints202503.2046.v1

57. Iacobas, D.A.; Iacobas, S.; Stout, R.F.; Spray, D.C. Cellular Environment Remodels the Genomic Fabrics of Functional Pathways in Astrocytes. *Genes (Basel).* **2020**; 11(5):520. doi: 10.3390/genes11050520.
58. Wang, Y.; Peng J, Bai, S.; Yu, H.; He, H.; Fan, C.; Hao, Y.; Guan, Y. A PIK3R2 Mutation in Familial Temporal Lobe Epilepsy as a Possible Pathogenic Variant. *Front Genet.* **2021**; 12:596709. doi: 10.3389/fgene.2021.596709.
59. Ge, J.; Jiao, X.; Li, H. MicroRNA-126-3P targets PIK3R2 to ameliorate autophagy and apoptosis of cortex in hypoxia-reoxygenation treated neonatal rats. *Cell Mol Biol* (Noisy-le-grand). **2023**; 69(12):210-217. doi: 10.14715/cmb/2023.69.12.34.
60. Feng, Y.; Wei, Z.H.; Liu, C.; Li, G.Y.; Qiao, X.Z.; Gan, Y.J.; Zhang, C.C.; Deng, Y.C. Genetic variations in GABA metabolism and epilepsy. *Seizure*. **2022**; 101:22-29. doi: 10.1016/j.seizure.2022.07.007.
61. Xie, M.; Qin, H.; Liu, L.; Wu, J.; Zhao, Z.; Zhao, Y.; Fang, Y.; Yu, X.; Su, C. GABA regulates metabolic reprogramming to mediate the development of brain metastasis in non-small cell lung cancer. *J Exp Clin Cancer Res*. **2025**; 44(1):61. doi: 10.1186/s13046-025-03315-9.
62. Wang, J.; Wang, X.; Yang, J.; Zhen, Y.; Ban, W.; Zhu, G. Molecular profiling of a rat model of vascular dementia: Evidences from proteomics, metabolomics and experimental validations. *Brain Res.* **2025**; 1846:149254. doi: 10.1016/j.brainres.2024.149254. Epub 2024 Sep 26.
63. Zheng, C.; Zhao, Y.; Hu, C.; Zhang, L.; Li, G.; Yang, C. Transcriptomic and network analysis identifies shared pathways across Alzheimer's disease and vascular dementia. *Brain Res*. **2025**; 1854:149548. doi: 10.1016/j.brainres.2025.149548. Epub ahead of print. PMID: 40043785.
64. Kilic-Berkmen, G.; Scorr, L.M.; McKay, L.; Thayani, M.; Donsante, Y.; Perlmutter, J.S.; Norris, S.A.; Wright, L.; Klein, C.; Feuerstein, J.S. et al. Sex Differences in Dystonia. *Mov Disord Clin Pract*. **2024**; 11(8):973-982. doi: 10.1002/mdc3.14059.
65. Abeledo-Machado, A.; Peña-Zanoni, M.; Bornancini, D.; Camilletti, M.A.; Faraoni, E.Y.; Marcial, A.; Rulli, S.; Alhenc-Gelas, F.; Díaz-Torga, G.S. Sex-specific Regulation of Prolactin Secretion by Pituitary Bradykinin Receptors. *Endocrinology*. **2022**; *163*(9):bqac108. doi: 10.1210/endocr/bqac108.
66. Smith, B.S.; Diaguarachchige De Silva, K.H.; Hashemi, A.; Duncan, R.E.; Grapentine, S.; Bakovic, M.; Lu, R. Transcription factor CREB3 is a potent regulator of high-fat diet-induced obesity and energy metabolism. *Int J Obes* (Lond). **2022**; *46(8):1446-1455. doi: 10.1038/s41366-022-01128-w.*
67. Deluca, A.; Bascom, B.; Key Planas, D.A.; Kocher, M.A.; Torres, M.; Arbeitman, M.N. Contribution of neurons that express fruitless and Clock transcription factors to behavioral rhythms and courtship. *iScience*. **2025**; *28(3)*:112037. doi: 10.1016/j.isci.2025.112037.
68. Towers, E.B.; Kilgore, M.; Bakhti-Suroosh, A.; Pidaparthi, L.; Williams, I.L.; Abel, J.M.; Lynch, W.J. Sex differences in the neuroadaptations associated with incubated cocaine-craving: A focus on the dorsomedial prefrontal cortex. *Front Behav Neurosci*. **2023**; *16*:1027310. doi: 10.3389/fnbeh.2022.1027310.
69. Eskow Jaunarajs, K.L.; Scarduzio, M.; Ehrlich, M.E.; McMahon, L.L.; Standaert, D.G. Diverse Mechanisms Lead to Common Dysfunction of Striatal Cholinergic Interneurons in Distinct Genetic Mouse Models of Dystonia. *J Neurosci*. **2019**; *39(36)*:7195-7205. doi: 10.1523/JNEUROSCI.0407-19.2019.
70. Daubner, S.C.; Le, T.; Wang, S. Tyrosine hydroxylase and regulation of dopamine synthesis. *Arch Biochem Biophys* **2011**, *508*, 1-12, doi:10.1016/j.abb.2010.12.017.
71. Chen, W.; Byun, J.; Kang, H.C.; Lee, H.S.; Lee, J.Y.; Kwon, Y.J.; Cho, Y.Y. Karyoptosis as a novel type of UVB-induced regulated cell death. *Free Radic Res* **2024**, *58*, 796-810, doi:10.1080/10715762.2024.2433986.
72. Zhang, Y.; Shi, Y.; Tang, J.; Chen, K.; Wu, M.; Wu, X.; Qiu, X. A transcriptomics-based analysis of mechanisms involved in the sex-dependent effects of diazepam on zebrafish. *Aquat Toxicol* **2024**, *275*, 107063, doi:10.1016/j.aquatox.2024.107063.
73. Yotova, A.Y.; Li, L.L.; O'Leary, A.; Tegeder, I.; Reif, A.; Courtney, M.J.; Slattery, D.A.; Freudenberg, F. Synaptic proteome perturbations after maternal immune activation: Identification of embryonic and adult hippocampal changes. *Brain Behav Immun* **2024**, *121*, 351-364, doi:10.1016/j.bbi.2024.07.040.
74. Peng, J.; Wang, Y.; He, F.; Chen, C.; Wu, L.W.; Yang, L.F.; Ma, Y.P.; Zhang, W.; Shi, Z.Q.; Chen, C.; et al. Novel West syndrome candidate genes in a Chinese cohort. *CNS Neurosci Ther* **2018**, *24*, 1196-1206, doi:10.1111/cns.12860.

 doi:10.20944/preprints202503.2046.v1

75. Gray, A.L.; Hyde, T.M.; Deep-Soboslay, A.; Kleinman, J.E.; Sodhi, M.S. Sex differences in glutamate receptor gene expression in major depression and suicide. *Mol Psychiatry* **2015**, *20*, 1057-1068, doi:10.1038/mp.2015.91.
76. Kipnis, P.A.; Sullivan, B.J.; Kadam, S.D. Sex-Dependent Signaling Pathways Underlying Seizure Susceptibility and the Role of Chloride Cotransporters. *Cells* **2019**, *8*, doi:10.3390/cells8050448.
77. Philibert, C.E.; Garcia-Marcos, M. Smooth operator(s): dialing up and down neurotransmitter responses by G-protein regulators. *Trends Cell Biol* **2024**, doi:10.1016/j.tcb.2024.07.002.
78. Gonzalez-Hernandez, A.J.; Munguba, H.; Levitz, J. Emerging modes of regulation of neuromodulatory G protein-coupled receptors. *Trends Neurosci* **2024**, *47*, 635-650, doi:10.1016/j.tins.2024.05.008.
79. Berridge, M.J.; Lipp, P.; Bootman, M.D. The versatility and universality of calcium signalling. *Nat Rev Mol Cell Biol* **2000**, *1*, 11-21, doi:10.1038/35036035.
80. Iacobas, D.A.; Suadicani, S.O.; Spray, D.C.; Scemes, E. A stochastic two-dimensional model of intercellular Ca2+ wave spread in glia. *Biophys J* **2006**, *90*, 24-41, doi:10.1529/biophysj.105.064378.
81. Zakharyan, R.; Atshemyan, S.; Boyajyan, A. Risk and protective effects of the complexin-2 gene and gene-environment interactions in schizophrenia. *Recent Adv DNA Gene Seq*. **2014**; 8(1):30-4. doi: 10.2174/1872215608666141001153202.
82. Anderson, E.M.; Loke, S.; Wrucke, B.; Engelhardt, A.; Demis, S.; O'Reilly, K.; Hess, E.; Wickman, K.; Hearing, M.C. Suppression of pyramidal neuron G protein-gated inwardly rectifying K+ channel signaling impairs prelimbic cortical function and underlies stress-induced deficits in cognitive flexibility in male, but not female, mice. *Neuropsychopharmacology*. **2021**; 46(12):2158-2169. doi: 10.1038/s41386-021-01063-w.
83. Chen, Q.; Kou, H.; Demy, D.L.; Liu, W.; Li, J.; Wen, Z.; Herbomel, P.; Huang, Z.; Zhang, W.; Xu, J. The different roles of V-ATPase a subunits in phagocytosis/endocytosis and autophagy. *Autophagy*. **2024**; 20(10):2297-2313. doi: 10.1080/15548627.2024.2366748.
84. Prinslow, E.A.; Stepien, K.P.; Pan, Y.Z.; Xu, J.; Rizo, J. Multiple factors maintain assembled trans-SNARE complexes in the presence of NSF and alphaSNAP. *Elife* **2019**, *8*, doi:10.7554/eLife.38880.
85. Gao, Y.; Ma, L.; Yuan, J.; Huang, Y.; Ban, Y.; Zhang, P.; Tan, D.; Liang, M.; Li, Z.; Gong, C.; Xu, T. et al. GLS2 reduces the occurrence of epilepsy by affecting mitophagy function in mouse hippocampal neurons. *CNS Neurosci Ther*. **2024**; 30(10):e70036. doi: 10.1111/cns.70036.
86. Gauthier, M.; Hebert, L.P.; Dugast, E.; Lardeux, V.; Letort, K.; Thiriet, N.; Belnoue, L.; Balado, E.; Solinas, M.; Belujon, P. Sex-dependent effects of stress on aIC-NAc circuit neuroplasticity: Role of the endocannabinoid system. *Prog Neuropsychopharmacol Biol Psychiatry*. **2025**; 138:111335. doi: 10.1016/j.pnpbp.2025.111335.
87. Sazhina, T, Tsurugizawa T, Mochizuki Y, Saito A, Joji-Nishino A, Ouchi K, Yagishita S, Emoto K, Uematsu A. Time- and sex-dependent effects of juvenile social isolation on mouse brain morphology. Neuroimage. 2025 Mar 4;310:121117. doi: 10.1016/j.neuroimage.2025.121117.
88. Wei, A.; Zhao, A.; Zheng, C.; Dong, N.; Cheng, X.; Duan, X.; Zhong, S.; Liu, X.; Jian, J.; Qin, Y. et al. Sexually dimorphic dopaminergic circuits determine sex preference. *Science*. **2025**; 387(6730):eadq7001. doi: 10.1126/science.adq7001.
89. Sangu, N.; Shimojima, K.; Takahashi, Y.; Ohashi, T.; Tohyama, J.; Yamamoto, T. A 7q31.33q32.1 microdeletion including LRRC4 and GRM8 is associated with severe intellectual disability and characteristics of autism. *Hum Genome Var*. **2017**; 4:17001. doi: 10.1038/hgv.2017.1.
90. Friedman, D.; Kannan, K.; Faustin, A.; Shroff, S.; Thomas, C.; Heguy, A.; Serrano, J.; Snuderl, M.; Devinsky, O. Cardiac arrhythmia and neuroexcitability gene variants in resected brain tissue from patients with sudden unexpected death in epilepsy (SUDEP). *NPJ Genom Med*. **2018**; 3:9. doi: 10.1038/s41525-018-0048-5.
91. Liu, J.; Tang, F.; Hu, D.; Zhang, Z.; Yan, Y.; Ma, Y. TMT-based proteomics profile reveals changes of the entorhinal cortex in a kainic acid model of epilepsy in mice. *Neurosci Lett*. **2023**; 800:137127. doi: 10.1016/j.neulet.2023.137127.
92. Wu, B.; Chen, X.; Pan, X.; Deng, X.; Li, S.; Wang, Z.; Wang, J.; Liao, D.; Xu, J.; Chen, M. et al. Single-cell transcriptome analyses reveal critical roles of RNA splicing during leukemia progression. *PLoS Biol*. **2023**; 21(5):e3002088. doi: 10.1371/journal.pbio.3002088.

93. Keustermans, G.C.; Kofink, D.; Eikendal, A.; de Jager, W.; Meerding, J.; Nuboer, R.; Waltenberger, J.; Kraaijeveld, A.O.; Jukema, J.W.; Sels, J.W. et al. Monocyte gene expression in childhood obesity is associated with obesity and complexity of atherosclerosis in adults. *Sci Rep*. **2017**; 7(1):16826. doi: 10.1038/s41598-017-17195-3.
94. Iacobas, D.A.; Tuli, N.Y.; Iacobas, S.; Rasamny, J.K.; Moscatello, A.; Geliebter, J.; Tiwari, R.K. Gene master regulators of papillary and anaplastic thyroid cancers. *Oncotarget* **2018**, *9*, 2410-2424, doi:10.18632/oncotarget.23417.
95. Schwehn, P.M., Falter-Braun, P. Inferring protein from transcript abundances using convolutional neural networks. *BioData Mining* **2025** *18*. https://doi.org/10.1186/s13040-025-00434-z
96. Mekic, R.; Zolotovskaia, M.A.; Sorokin, M.; Mohammad, T.; Shaban, N.; Musatov, I.; Tkachev, V.; Modestov, A.; Simonov, A.; Kuzmin, D. et al. Number of human protein interactions correlates with structural, but not regulatory conservation of the respective genes. *Front Genet*. **2024**; 15:1472638. doi: 10.3389/fgene.2024.1472638.
97. Xie, J.; Wang, J.; Cui, X. Research progress on estrogen and estrogen receptors in the occurrence and progression of autoimmune thyroid diseases. *Autoimmun Rev*. **2025**; 24(6):103803. doi: 10.1016/j.autrev.2025.103803. Epub ahead of print.
98. Aten, S.; Ramirez-Plascencia, O.; Blake, C.; Holder, G.; Fishbein, E.; Vieth, A.; Zarghani-Shiraz, A.; Keister, E.; Howe, S.; Appo, A. et al. A time for sex: circadian regulation of mammalian sexual and reproductive function. *Front Neurosci*. **2025**; 18:1516767. doi: 10.3389/fnins.2024.1516767.
99. Iacobas, D.A.; Iacobas, S.; Nebieridze, N.; Velíšek, L.; Velíšková, J. Estrogen Protects Neurotransmission Transcriptome During Status Epilepticus. *Front Neurosci*. **2018**; 12:332. doi: 10.3389/fnins.2018.00332.
100. Huang, S.; Shi, C.; Tao, D.; Yang, C.; Luo, Y. Modulating reward and aversion: Insights into addiction from the paraventricular nucleus. *CNS Neurosci Ther* **2024**, *30*, e70046, doi:10.1111/cns.70046.
101. Xing, M.; Li, Y.; Zhang, Y.; Zhou, J.; Ma, D.; Zhang, M.; Tang, M.; Ouyang, T.; Zhang, F.; Shi, X.; et al. Paraventricular hypothalamic RUVBL2 neurons suppress appetite by enhancing excitatory synaptic transmission in distinct neurocircuits. *Nat Commun* **2024**, *15*, 8939, doi:10.1038/s41467-024-53258-6.
102. Griffin, H.; Hanson, J.; Phelan, K.D.; Baldini, G. MC4R Localizes at Excitatory Postsynaptic and Peri-Postsynaptic Sites of Hypothalamic Neurons in Primary Culture. *Cells* **2024**, *13*, doi:10.3390/cells13151235.
103. Iacobas, D.A.; Iacobas, S.; Thomas, N.; Spray, D.C. Sex-dependent gene regulatory networks of the heart rhythm. *Funct Integr Genomics* **2010**, *10*, 73-86, doi:10.1007/s10142-009-0137-8.
104. Iacobas, S.; Amuzescu, B.; Iacobas, D.A. Transcriptomic uniqueness and commonality of the ion channels and transporters in the four heart chambers. *Sci Rep* **2021**, *11*, 2743, doi:10.1038/s41598-021-82383-1.
105. Iacobas, D.A.; Fan, C.; Iacobas, S.; Spray, D.C.; Haddad, G.G. Transcriptomic changes in developing kidney exposed to chronic hypoxia. *Biochem Biophys Res Commun* **2006**, *349*, 329-338, doi:10.1016/j.bbrc.2006.08.056.